First Wall Mechanical Design for Light Ion Beam Fusion Reactors

R.L. Engelstad and E.G. Lovell

December 1979

UWFDM-322

FUSION TECHNOLOGY INSTITUTE

UNIVERSITY OF WISCONSIN

MADISON WISCONSIN

First Wall Mechanical Design for Light Ion Beam Fusion Reactors

R.L. Engelstad and E.G. Lovell

Fusion Technology Institute
University of Wisconsin
1500 Engineering Drive
Madison, WI 53706

http://fti.neep.wisc.edu

December 1979

UWFDM-322

FIRST WALL MECHANICAL DESIGN FOR LIGHT ION BEAM FUSION REACTORS

Roxann L. Engelstad

Edward G. Lovell

ABSTRACT

Techniques are developed for the determination of the response of LIB fusion reactor wall structures from internal blast pressure. Plate-like components of both solid and cellular geometries are analyzed using equivalent models with appropriate dynamic load factors. Parametric curves are presented for the determination of physical dimensions for prescribed deflection and stress limits or vice-versa. Sample calculations show that a range of practical values are possible for the design of such reactor containment structures.

UWFDM-322

I. INTRODUCTION

The design of the containment vessel of a light ion beam fusion reactor is influenced by a number of considerations. For structural design purposes, the major load source is the repetitive blast wave impinging on the first wall. Because of the symmetric nature of this source, a structural configuration which generally has spherical characteristics would be natural and most practical.

In the work which follows, a conceptual ribbed shell is modelled. Since there should be no difficulty with the design of ribs and associated supporting members, the analysis focuses on subpanels of the structural system. Design methods are developed for determining dimensions and estimating stresses, deflections, and vibrational frequencies resulting from the internal dynamic pressure pulse.

LIGHT ION BEAM REACTOR CAVITY AND FIRST WALL

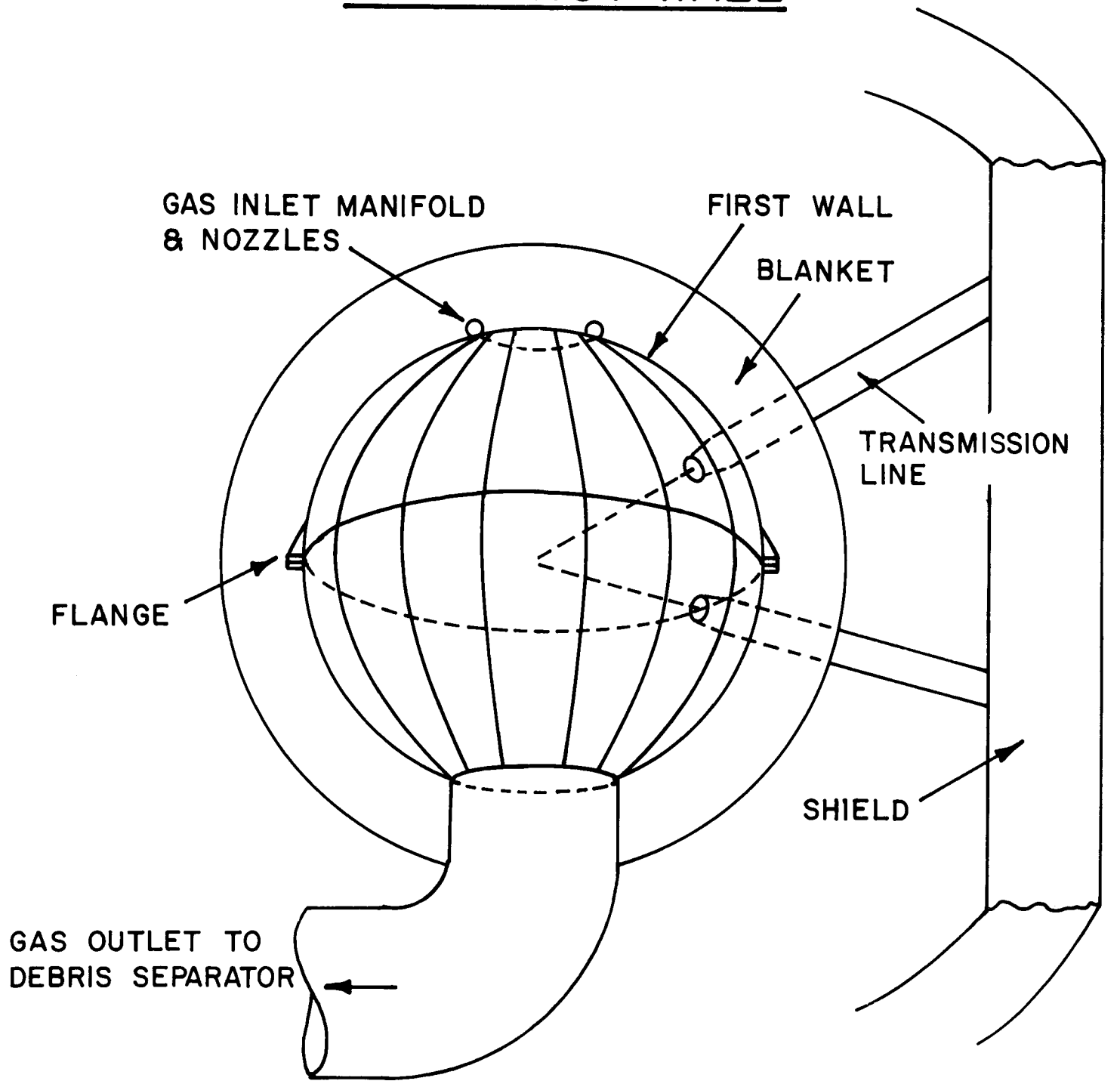

FIGURE 1

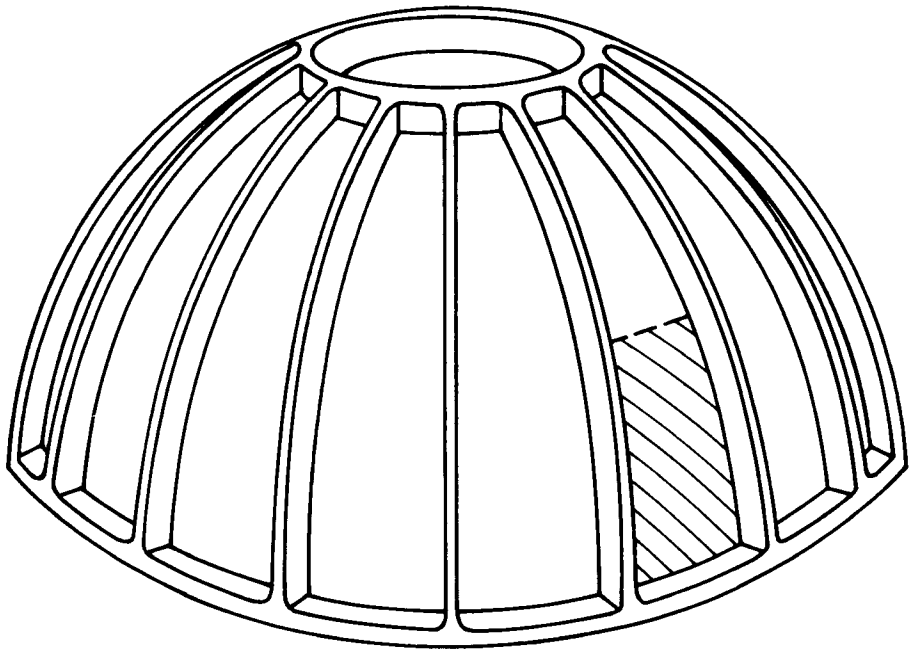

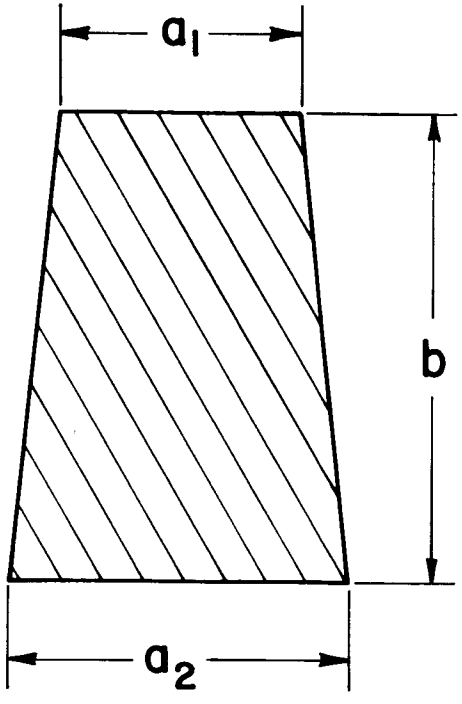

CONCEPTUAL REPRESENTATION OF MERIDIONAL RIB STIFFENING AND TRAPEZOIDAL SUB-PANEL.

FIGURE 2

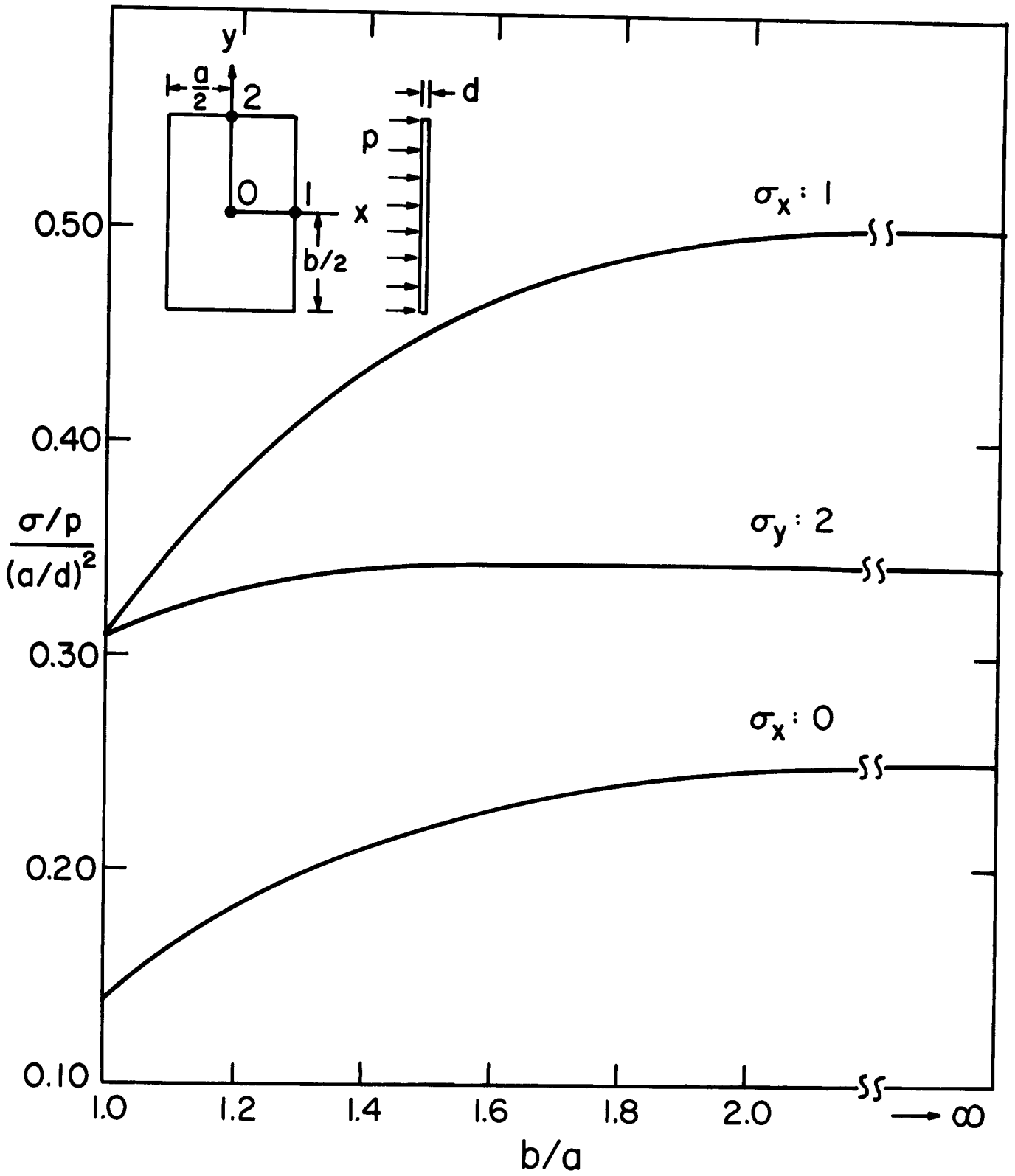

DIMENSIONLESS STATIC STRESS VS. ASPECT RATIO

FIGURE 3

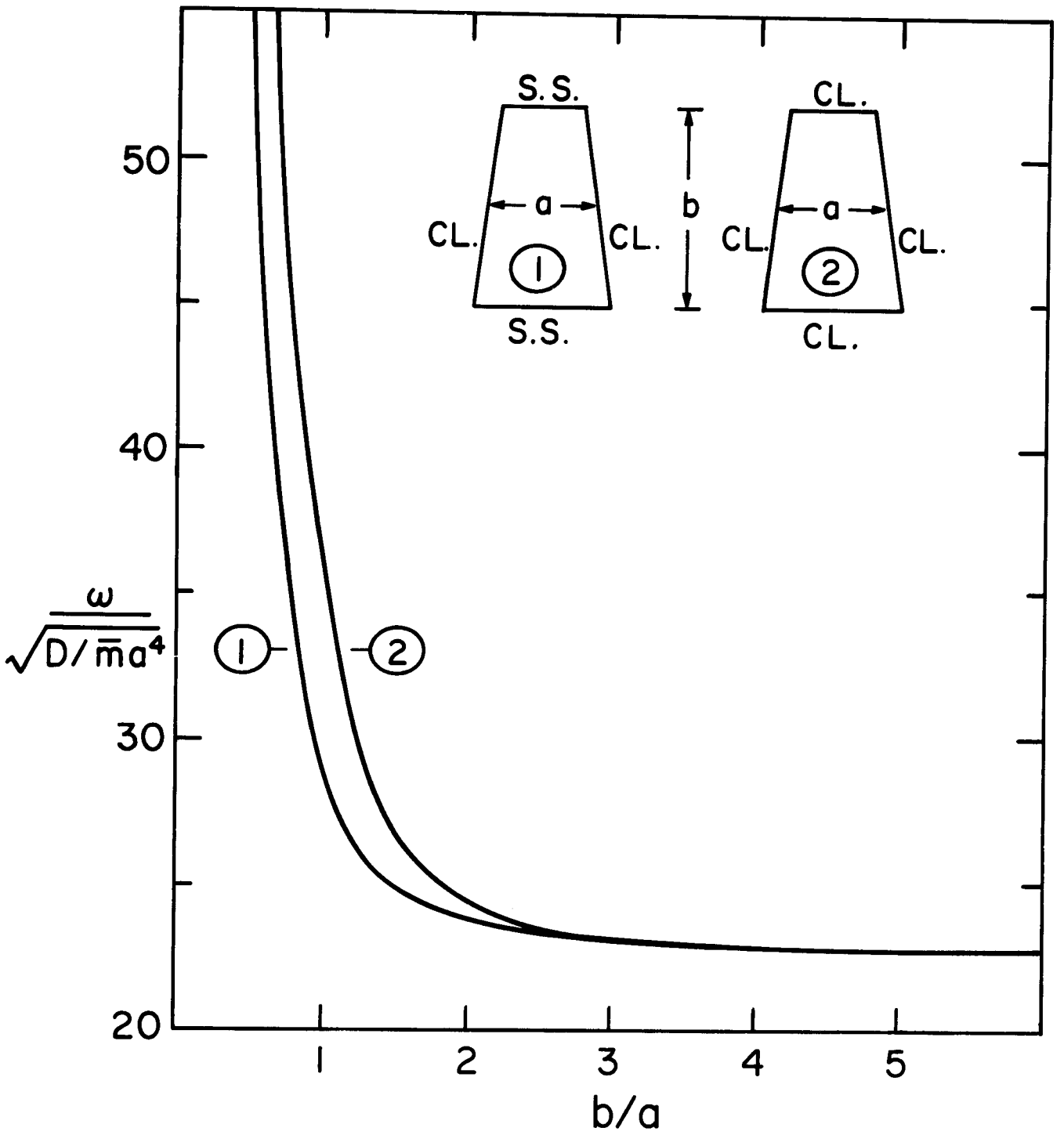

FUNDAMENTAL FREQUENCY VS. ASPECT RATIO FOR AN EQUIVALENT SOLID PLATE

FIGURE 4

legitimate simplifying approximations can be employed for determining the frequencies and flexural stresses.

II.2 Cellular Wall Simplifications

For static or dynamic pressure loadings, stresses and deflections may be reduced by increasing flexural stiffness. This can be achieved without a weight penalty by using a sandwich construction. In this application a cellular plate (Figure 5) will allow internal coolant flow with the webbing carrying shear, separating the plate faces and serving as a portion of the tubular wall. Generally because principal stiffnesses are different, such a plate should be considered orthotropic. However it is felt that the error resulting from neglecting such orthotropy would be acceptable in this preliminary design. For such purposes, Figure 5 shows the difference in principal stiffnesses, expressed as a percentage of the greater value for different geometric parameters. As an example, for a cell which is essentially square and a wall thickness one tenth of the face spacing, this difference is approximately ten percent.

II.3 Dynamic Load Factor

One approach to the dynamic analysis of plates consists of determining the quasi-static reaction and multiplying it by a dynamic load factor (DLF) to give corresponding dynamic effects[3]. The dynamic load factor is defined as the ratio of the dynamic response to the static response. Since deflections and stresses in the plate are proportional, the dynamic load factor may be used in either. For example, using displacements as a response

$$DLF = x/x_{st} .$$

Since a plate, under uniform impulsive pressure, will respond

DIFFERENCE IN PRINCIPAL FLEXURAL STIFFNESSES AS A FUNCTION OF CELL GEOMETRY

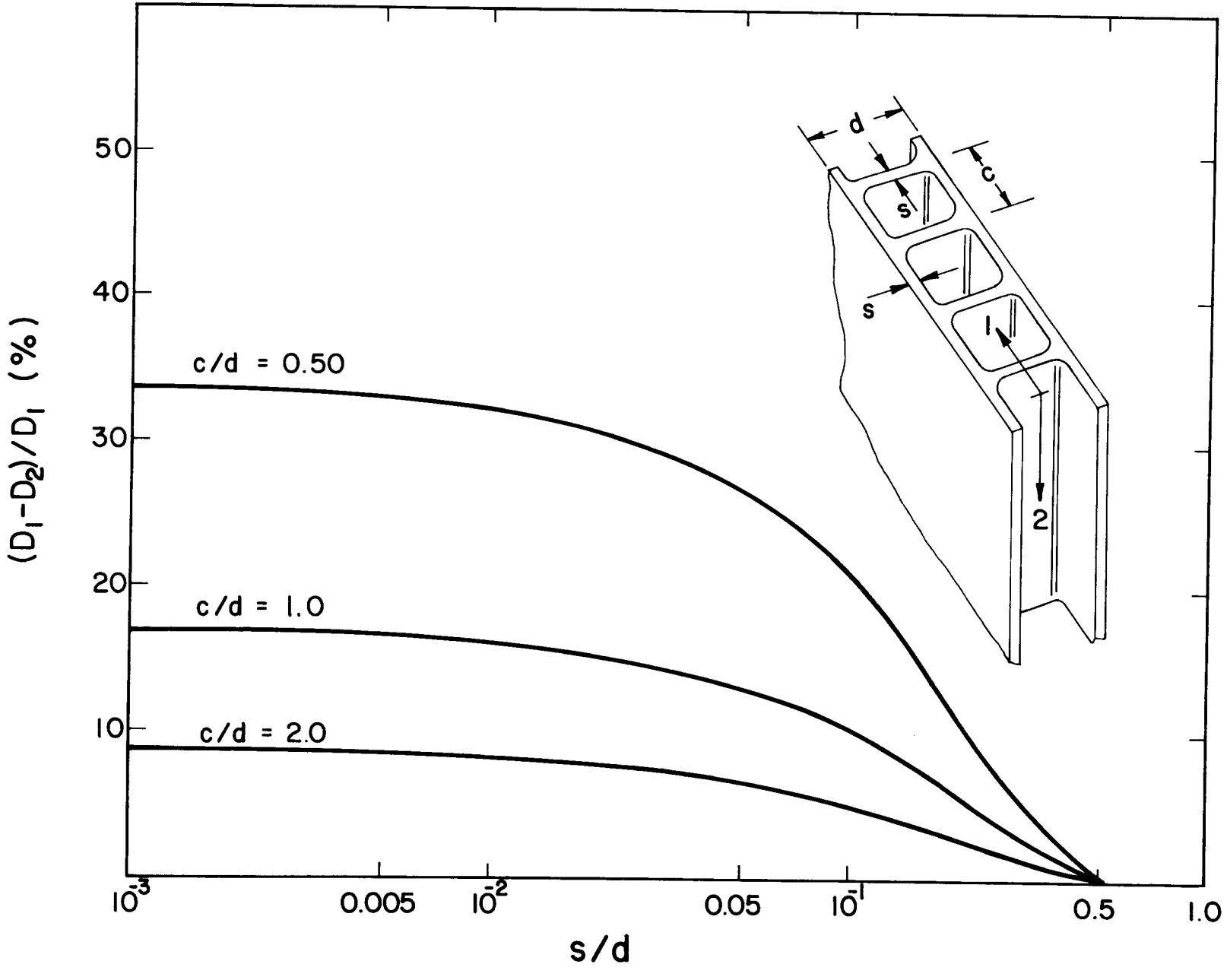

FIGURE 5

approximately as a single-degree-of-freedom system, the results of such a system can be used to simplify the dynamic analysis. Consider the response of the linear undamped system shown in Figure 6

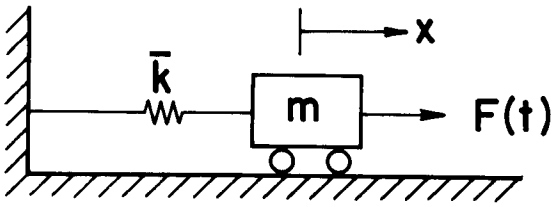

Figure 6

where $F(t)$ is the excitation, a prescribed function of time. The governing differential equation of motion is given by

$$m\ddot{x} + \bar{k}x = F(t) .$$

For the homogeneous solution,

$$x_H = x_o \cos \omega t + \frac{\dot{x}_o}{\omega} \sin \omega t$$

where x_o and $\dot{x}_o$ are the initial displacement and velocity, respectively, and ω is the natural frequency.

For the particular solution, consider the general load-time function shown in Figure 7.

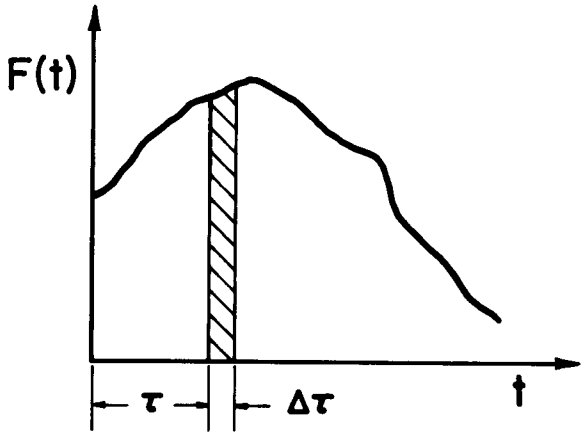

Figure 7

Let the shaded area shown represent an impulse applied at time $t = \tau$. The change in displacement due to this impulse is

$$\Delta x = \frac{F(\tau)\ \Delta\tau}{m\omega} \sin \omega(t-\tau) \quad .$$

If the entire excitation function is considered as a large number of impulses, the total displacement after time t would be given by

$$x = \int_0^t \frac{F(\tau)}{m\omega} \sin \omega(t-\tau)\, d\tau \quad .$$

With $F(\tau) = F_{max} f(\tau)$, the static deflection is

$$x_{st} = \frac{F_{max}}{\bar{k}} = \frac{F_{max}}{m\omega^2} \quad .$$

Substituting this into the response

$$x_p = x_{st}\, \omega \int_0^t f(\tau) \sin \omega(t-\tau)\, d\tau \; ^* \quad .$$

Now, the complete solution is given by

$$x = x_H + x_p$$

or,

$$x = x_o \cos \omega t + \frac{\dot{x}_o}{\omega} \sin \omega t + x_{st}\omega \int_0^t f(\tau) \sin \omega(t-\tau)\, d\tau \quad .$$

For the chamber wall design, a pressure-blast pulse is used for $f(\tau)$. Consider the load function to consist of a ramp with rise time t_r followed by an exponential decay (Figure 8).

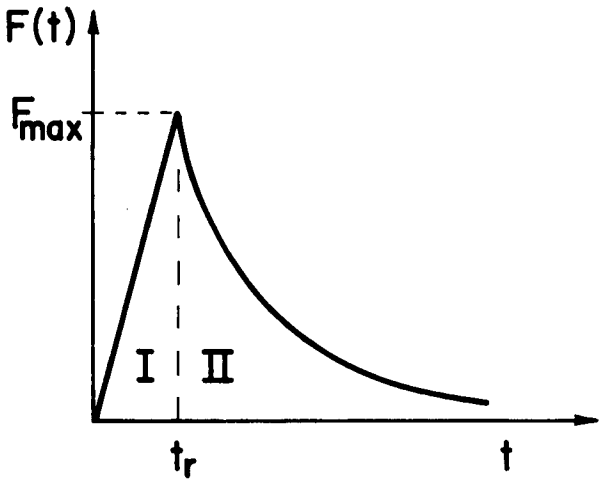

Figure 8

Interval I:

$$\tau \leq t_r \qquad f(\tau) = \frac{\tau}{t_r}$$

Interval II:

$$\tau > t_r \qquad f(\tau) = e^{-k(\tau - t_r)}$$

---

*Duhamel's integral.

For the first interval the initial displacement and velocity are zero. Then after integration, the response becomes,

$$x = \frac{x_{st}}{t_r}\left[t - \frac{\sin \omega t}{\omega}\right]$$

or,

$$DLF = \frac{1}{t_r}\left[t - \frac{\sin \omega t}{\omega}\right] .$$

For the second interval, x_o and $\dot{x}_o$ can be found from the preceeding results.

$$x_o = \frac{x_{st}}{t_r}\left[t_r - \frac{\sin \omega t_r}{\omega}\right]$$

$$\dot{x}_o = \frac{x_{st}}{t_r}\left[1 - \cos \omega t_r\right] .$$

Substituting these values into the expression for the complete response and performing the integration gives

$$x = \frac{x_{st}}{t_r}\left[t_r - \frac{\sin \omega t_r}{\omega}\right] \cos \omega t + \frac{x_{st}}{\omega t_r}\left[1 - \cos \omega t_r\right] \sin \omega t$$

$$+ \frac{x_{st}\omega}{k^2+\omega^2}\left[\omega e^{-k(t-t_r)} + k \sin \omega(t-t_r) - \omega \cos \omega(t-t_r)\right]$$

where $t > t_r$. Simplifying this expression and dividing through by x_{st} results in

$$DLF = \left[\frac{k^2/\omega^2}{1 + k^2/\omega^2} - \frac{\sin \omega t_r}{\omega t_r}\right] \cos \omega(t-t_r)$$

$$+ \left[\frac{k/\omega}{1 + k^2/\omega^2} + \frac{1 - \cos \omega t_r}{\omega t_r}\right] \sin \omega(t-t_r)$$

$$+ \frac{e^{-k(t-t_r)}}{1 + k^2/\omega^2} \qquad t > t_r \quad .$$

III. ANALYSIS OF PANELS WITH CLAMPED MERIDIONAL EDGES

In this model, the slope and transverse deflection are zero on vertical edges ("clamped") while the deflection and resistance to rotation (flexural moment) are zero on the horizontal edges (simply supported).

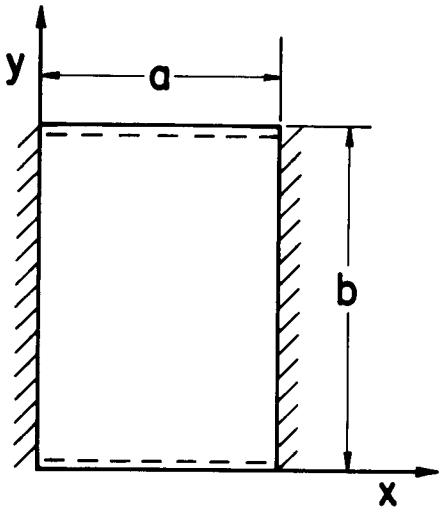

Figure 9

These boundary conditions can be expressed as

$$w(0,y) = w(a,x) = \frac{\partial w}{\partial x}(0,y) = \frac{\partial w}{\partial x}(a,y) = 0$$

$$w(x,0) = w(x,b) = \frac{\partial^2 w}{\partial y^2}(x,0) = \frac{\partial^2 w}{\partial y^2}(x,b) = 0$$

where w denotes the transverse displacement component. This deflection can be theoretically determined as accurately as required by a series, each term of which satisfies the given boundary conditions:

$$w(x,y) = \sum_{m=1}^{\infty} \sum_{n=1}^{\infty} W_{mn}\left(1 - \cos\frac{2m\pi x}{a}\right) \sin\frac{n\pi y}{b} \quad .$$

Modal shapes are defined by various combinations of m and n. However for problems of this type the response is well represented by the fundamental mode, i.e., when $m = n = 1$. Thus, the deflection surface is of the form

$$w = W_1\left(1 - \cos\frac{2\pi x}{a}\right) \sin\frac{\pi y}{b} \quad .$$

To obtain the modal equation of motion, Lagrange's work-energy equation is used:

$$\frac{d}{dt}\left(\frac{\partial K}{\partial \dot{W}_1}\right) + \frac{\partial U}{\partial W_1} = \frac{\partial \Omega_e}{\partial W_1}$$

where K = total kinetic energy

U = total flexural strain energy

Ω_e = external work.

The total kinetic energy for an element is given by

$$dK = \frac{1}{2}\,\bar{m}\,\dot{w}^2\,dxdy$$

where $\bar{m}$ = mass per unit area

$\dot{w}$ = time derivative of the displacement.

Integrating over the plate area

$$K = \frac{1}{2}\,\bar{m}\int_0^b\int_0^a \left[\dot{W}_1\left(1 - \cos\frac{2\pi x}{a}\right)\sin\frac{\pi y}{b}\right]^2 dxdy$$

$$= \frac{3}{8}\,\bar{m}\,ab\dot{W}_1^2 \quad .$$

Then,

$$\frac{d}{dt}\left(\frac{\partial K}{\partial \dot{W}_1}\right) = \frac{3}{4}\,\bar{m}\,ab\ddot{W}_1 \quad .$$

The total flexural strain energy is given by

$$U = \frac{D}{2}\int_0^b\int_0^a \left[\left(\frac{\partial^2 w}{\partial x^2}\right)^2 + \left(\frac{\partial w}{\partial y^2}\right)^2 + 2\nu\,\frac{\partial^2 w}{\partial x^2}\,\frac{\partial^2 w}{\partial y^2} + 2(1-\nu)\left(\frac{\partial^2 w}{\partial x \partial y}\right)^2\right] dxdy$$

where D is the plate flexural stiffness. For a solid plate it is defined as

$$D = Eh^3/12(1-\nu^2)$$

with h and ν denoting the thickness and Poisson's ratio, respectively. Similarly for the cellular plate previously described, an effective stiffness is used[1]; thus

$$D = Esd^2/2(1-\nu^2)$$

where s and d are plate dimensions shown in Figure 4.

Integrating the strain energy,

$$U = \frac{D}{2} W_1^2 \pi^4 \left[\frac{3ab}{4b^4} + \frac{16ab}{4a^4} + \frac{8ab}{4a^2b^2}\right]$$

and

$$\frac{\partial U}{\partial W_1} = DW_1\pi^4 \left[\frac{3ab}{4b^4} + \frac{16ab}{4a^4} + \frac{8ab}{4a^2b^2}\right] .$$

The external work Ω_e is given by

$$\Omega_e = p(t) \int_0^b \int_0^a W_1 \left(1 - \cos \frac{2\pi x}{a}\right) \sin \frac{\pi y}{b} \, dxdy$$

$$= p(t) \, W_1 \frac{2ab}{\pi}$$

and

$$\frac{\partial \Omega_e}{\partial W_1} = p(t) \frac{2ab}{\pi} .$$

Substitution into the Lagrange equation produces

$$\frac{3}{4} \bar{m} ab\ddot{W}_1 + DW_1\pi^4 \left[\frac{3ab}{4b^4} + \frac{16ab}{4a^4} + \frac{8ab}{4a^2b^2}\right] = p(t) \frac{2ab}{\pi}$$

or

$$\ddot{W}_1 + \frac{D\pi^4}{3\bar{m}} \left[\frac{3}{b^4} + \frac{16}{a^4} + \frac{8}{a^2b^2}\right] W_1 = p(t) \frac{8}{3\bar{m}\pi} .$$

It can be noted from the above equation that the fundamental frequency is of the form

$$\omega_1 = \pi^2 \left[\frac{D}{3\bar{m}} \left(\frac{3}{b^4} + \frac{16}{a^4} + \frac{8}{a^2b^2}\right)\right]^{1/2} .$$

Thus, the equation of motion can be written as

$$\ddot{W}_1 + \omega_1^2 W_1 = p(t) 8/3\bar{m}\pi$$

where $p(t) = F_{max} f(t)$.

To find the static deflection w_{st}, the time dependency is eliminated in the preceeding equation producing

$$w_{st} = \frac{16F_{max}}{3\bar{m}\pi\omega_1^2} .$$

To approximate the dynamic response of the plate, it is necessary to multiply the static deflection by the dynamic load factor, i.e.,

$$w_{max} = w_{st}(DLF) .$$

The bending stresses, σ_x and σ_y, can also be directly determined from the deflection function w. For the solid plate,

$$\sigma_x = \frac{Eh}{2(1-\nu^2)} \left(\frac{\partial^2 w}{\partial x^2} + \nu \frac{\partial^2 w}{\partial y^2}\right)$$

$$= \frac{EhW_1\pi^2}{2(1-\nu^2)} \left[\frac{4}{a^2} \cos \frac{2\pi x}{a} - \frac{\nu}{b^2} \left(1 - \cos \frac{2\pi x}{a}\right)\right] \sin \frac{\pi y}{b}$$

$$\sigma_y = \frac{Eh}{2(1-\nu^2)} \left(\frac{\partial^2 w}{\partial y^2} + \nu \frac{\partial^2 w}{\partial x^2}\right)$$

$$= \frac{EhW_1\pi^2}{2(1-\nu^2)} \left[\frac{4\nu}{a^2} \cos \frac{2\pi x}{a} - \frac{1}{b^2} \left(1 - \cos \frac{2\pi x}{a}\right)\right] \sin \frac{\pi y}{b} .$$

For the given support conditions, maximum stresses will occur at the midspan of the clamped edges, i.e., $x = 0$ and $y = b/2$ or $x = a$ and $y = b/2$. Then, the bending stresses become

$$\sigma_{x_{max}} = \frac{EhW_1\pi^2}{2(1-\nu^2)} [4/a^2]$$

$$\sigma_{y_{max}} = \frac{EhW_1\pi^2}{2(1-\nu^2)} [4\nu/a^2] = \nu \sigma_{x_{max}}$$

with Poisson's ratio less than one, only $\sigma_{x_{max}}$ needs to be considered.

For the cellular plate, h must be replaced by the parameter d in the preceeding stress equations.

IV. ANALYSIS OF PANELS WITH SIMPLY SUPPORTED MERIDIONAL EDGES

In the analysis which follows, the plate is modeled as simply supported on all edges.

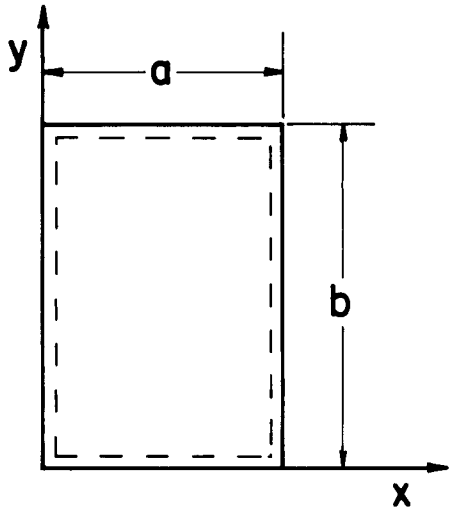

Figure 10

The boundary conditions are

$$w(x,0) = w(x,b) = w(0,y) = w(a,y) = 0$$

$$\frac{\partial^2 w}{\partial x^2}(0,y) = \frac{\partial^2 w}{\partial x^2}(a,y) = \frac{\partial^2 w}{\partial y^2}(x,0) = \frac{\partial^2 w}{\partial y^2}(x,b) = 0 \ .$$

To satisfy these boundary conditions a different deflection function must be used:

$$w(x,y) = \sum_{m=1}^{\infty} \sum_{n=1}^{\infty} W_{mn} \sin \frac{m\pi x}{a} \sin \frac{n\pi y}{b} \ .$$

Again, only the fundamental mode needs to be considered. Hence,

$$w = W_1 \sin \frac{\pi x}{a} \sin \frac{\pi y}{b} \ .$$

For this case, the Lagrange equation reduces to

$$\ddot{W}_1 + \frac{D\pi^4}{\bar{m}} \left(\frac{1}{a^2} + \frac{1}{b^2}\right)^2 W_1 = p(t) \frac{16}{\bar{m}\pi^2}$$

thus

$$\omega_1 = \pi^2 \sqrt{\frac{D}{\bar{m}}} \left(\frac{1}{a^2} + \frac{1}{b^2}\right) \ .$$

Rewriting the preceding equation of motion,

$$\ddot{W}_1 + \omega_1^2 W_1 = \frac{16p(t)}{\bar{m}\,\pi^2} = \frac{16F_{max}f(t)}{\bar{m}\,\pi^2}$$

where

$$w_{st} = \frac{16F_{max}}{\bar{m}\,\pi^2\omega_1^2}$$

and

$$w_{max} = w_{st}(DLF) \quad .$$

For the bending stresses, the displacement function $w(x,y)$ is again used. Then, for the solid plate

$$\sigma_x = \frac{EhW_1\pi^2}{2(1-\nu^2)}\left(\frac{1}{a^2} + \frac{\nu}{b^2}\right) \sin\frac{\pi x}{a} \sin\frac{\pi y}{b}$$

$$\sigma_y = \frac{EhW_1\pi^2}{2(1-\nu^2)}\left(\frac{1}{b^2} + \frac{\nu}{a^2}\right) \sin\frac{\pi x}{a} \sin\frac{\pi y}{b} \quad .$$

In this case, the maximum bending stress will occur at the center of the plate ($x = a/2$, $y = b/2$). Then these equations simplify to

$$\sigma_{x_{max}} = \frac{EhW_1\pi^2}{2(1-\nu^2)}\left(\frac{1}{a^2} + \frac{\nu}{b^2}\right)$$

$$\sigma_{y_{max}} = \frac{EhW_1\pi^2}{2(1-\nu^2)}\left(\frac{1}{b^2} + \frac{\nu}{a^2}\right) \quad .$$

Again $\sigma_{x_{max}}$ is the larger and will only be considered here.

For the cellular plate, the same stress equations are used with h replaced by the plate dimension d.

V. DESIGN CONSIDERATIONS

A comparison can be made of the mechanical response of stainless steel to zircaloy for the outside chamber wall. The relevant material properties are listed in Table 1.

TABLE 1

Material Properties

	Stainless Steel	Zircaloy
Density, $\rho(gm/cm^3)$	8.027	6.44
Elastic Modulus, $E(10^6$ psi)	28.0	11.0
Poisson's Ratio, ν	0.33	0.33

The loading used is the pressure-blast pulse given in Figure 11 from UWFDM-315[4] with ramp time of 0.2 milliseconds and the exponential constant k approximately 600/sec. If DLF versus time is to be plotted, the natural frequency ω must also be specified. As an example, in Figure 12, ω is given as 600 Hz and the DLF over a 5 millisecond span has been plotted. However, the relevant value to be obtained from this plot is the maximum DLF equal to 1.67. It is this maximum value that will correspond to the maximum response, which is needed in the design analysis. Figure 13 has DLF_{max} plotted versus ω for various values of k. The rise time has been left at 0.2 ms; however, a decrease in the rise time would result in lower DLF's.

In the two preceding analyses, equations were developed for frequencies, deflections, and stresses for clamped and simply supported plates. From these equations design curves have been developed to compare characteristics of plates made from the two metals.

A comparison can also be made between a solid and cellular plate. The analyses were the same for each except for the definition of the flexural rigidity. For the solid plate, D was given by

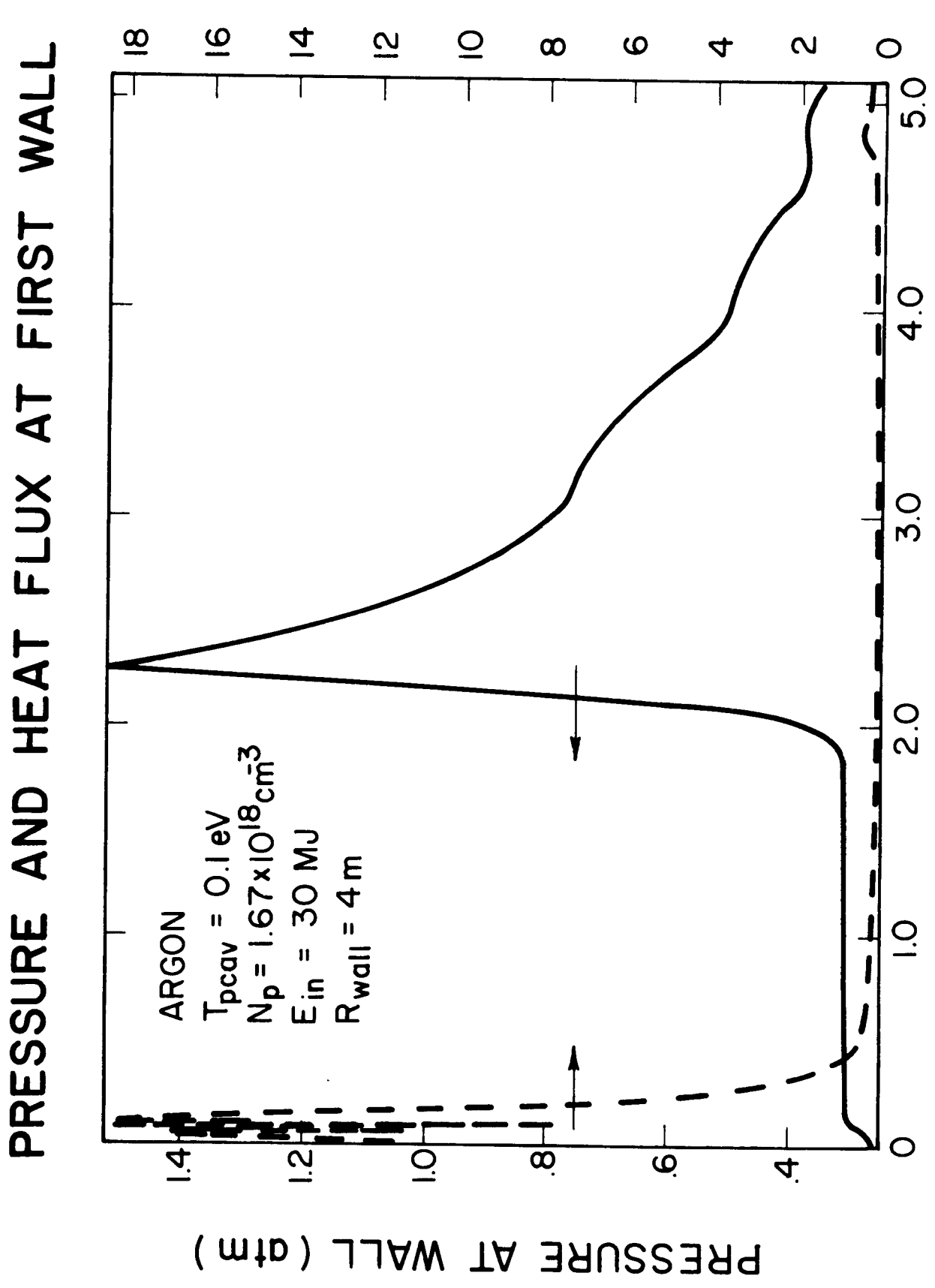
PRESSURE AND HEAT FLUX AT FIRST WALL
ARGON
T_{pcav} = 0.1 eV
N_p = 1.67×10^{18}cm^{-3}
E_{in} = 30 MJ
R_{wall} = 4 m
PRESSURE AT WALL (atm)
HEAT FLUX (kW/cm^2)
TIME (msec)
0
1.0
2.0
3.0
4.0
5.0
.4
.6
.8
1.0
1.2
1.4
0
2
4
6
8
10
12
14
16
18

FIGURE 11

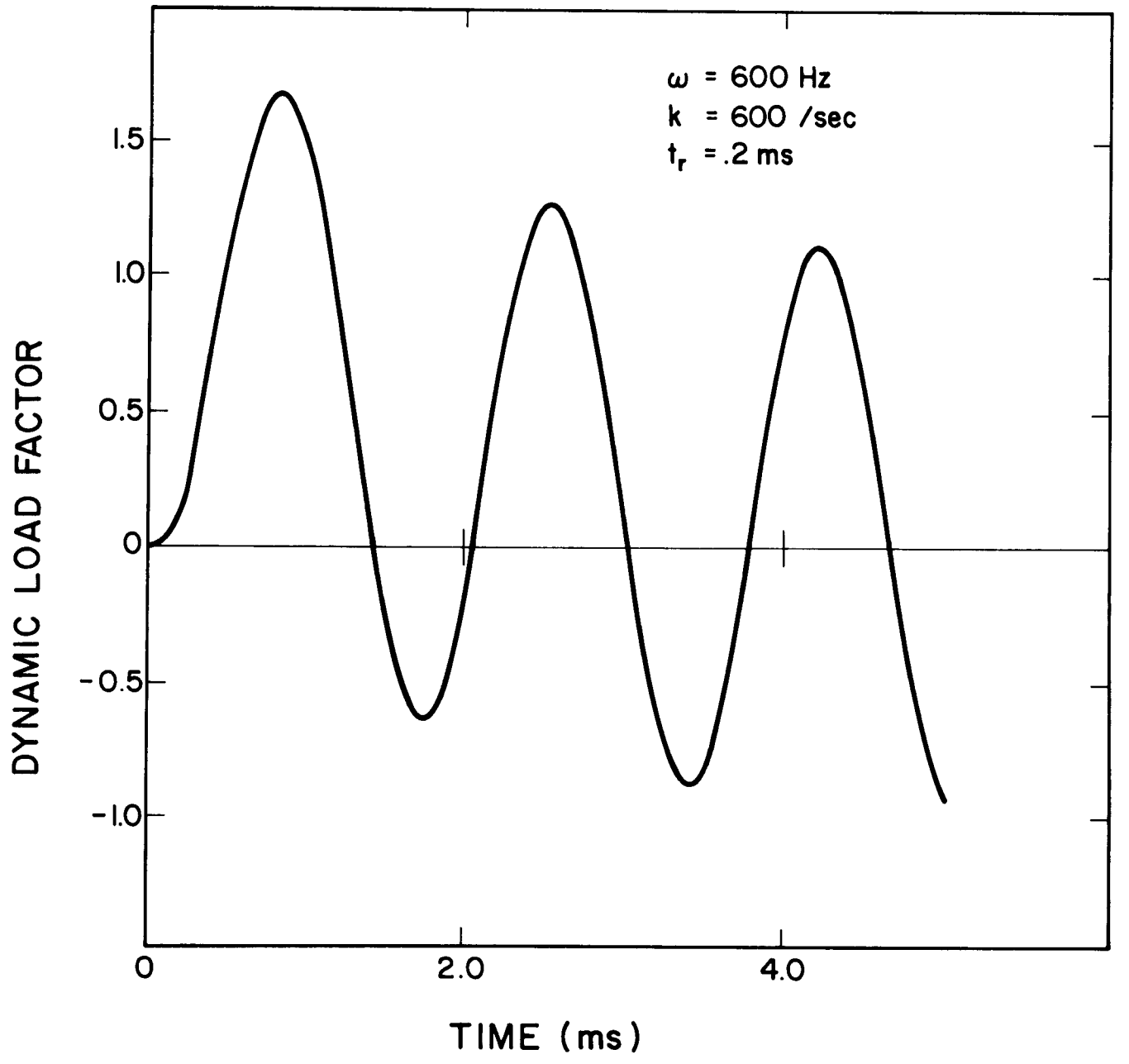
ω = 600 Hz
k = 600 /sec
t_r = .2 ms
DYNAMIC LOAD FACTOR
1.5
1.0
0.5
0
-0.5
-1.0
0
2.0
4.0
TIME (ms)

FIGURE 12

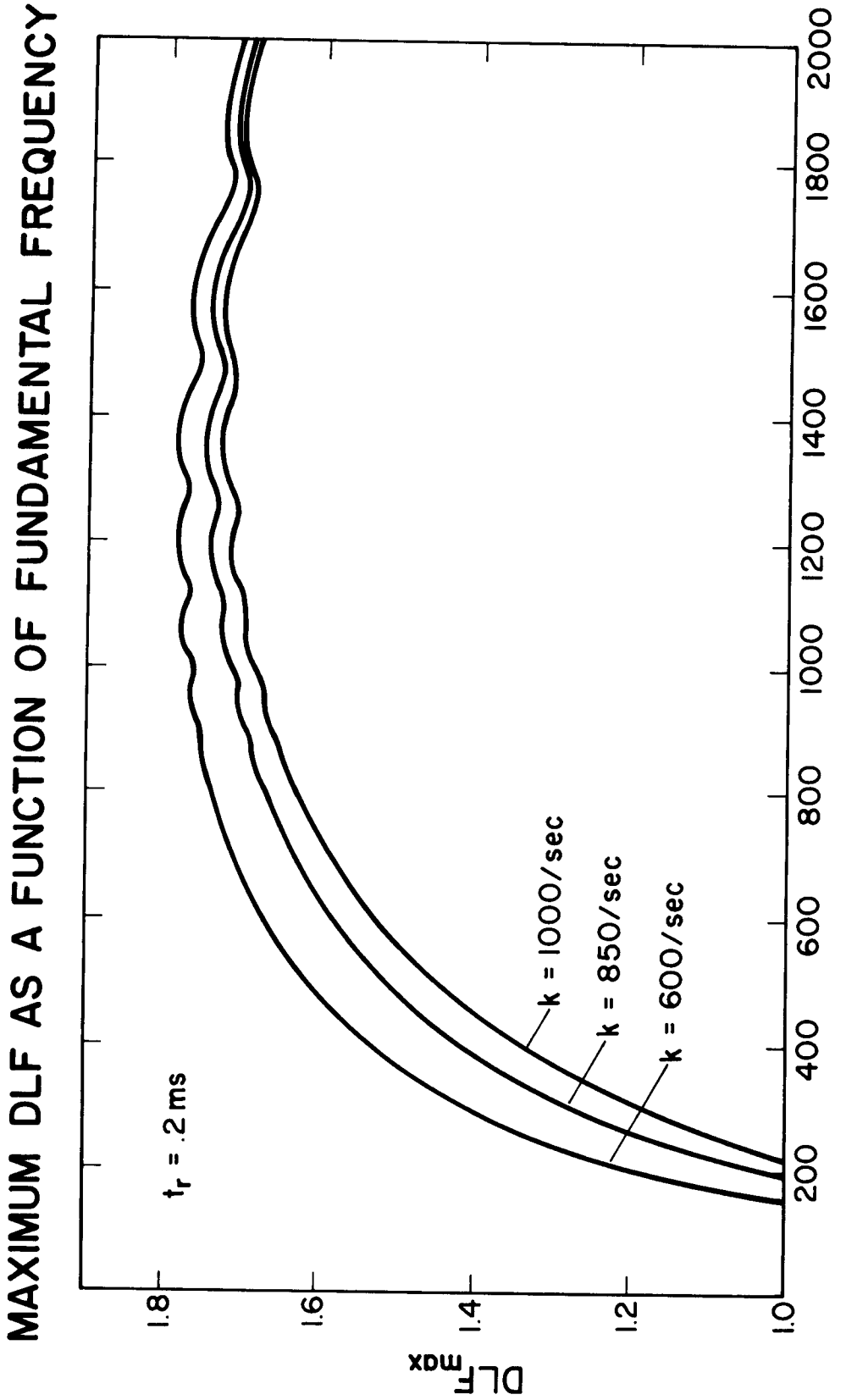
MAXIMUM DLF AS A FUNCTION OF FUNDAMENTAL FREQUENCY
DLF max
1.0
1.2
1.4
1.6
1.8
200
400
600
800
1000
1200
1400
1600
1800
2000
ω1 (HERTZ)
tr = .2 ms
k = 1000/sec
k = 850/sec
k = 600/sec

FIGURE 13

$$D = \frac{Eh^3}{12(1-\nu^2)}$$

and for the cellular plate,

$$D = \frac{Eth^2}{2(1-\nu^2)} \quad .$$

The mechanical response curves have been grouped according to the support conditions, i.e., Figures 14-23 are for clamped conditions, while Figures 24-33 represent simply supported conditions. Within each group are graphs for frequencies, deflections, and stresses for solid and cellular plates of both stainless steel and zircaloy. Methods for applying the information from the design curves have been outlined in the work that follows.

FUNDAMENTAL FREQUENCY AS A FUNCTION OF PLATE GEOMETRY

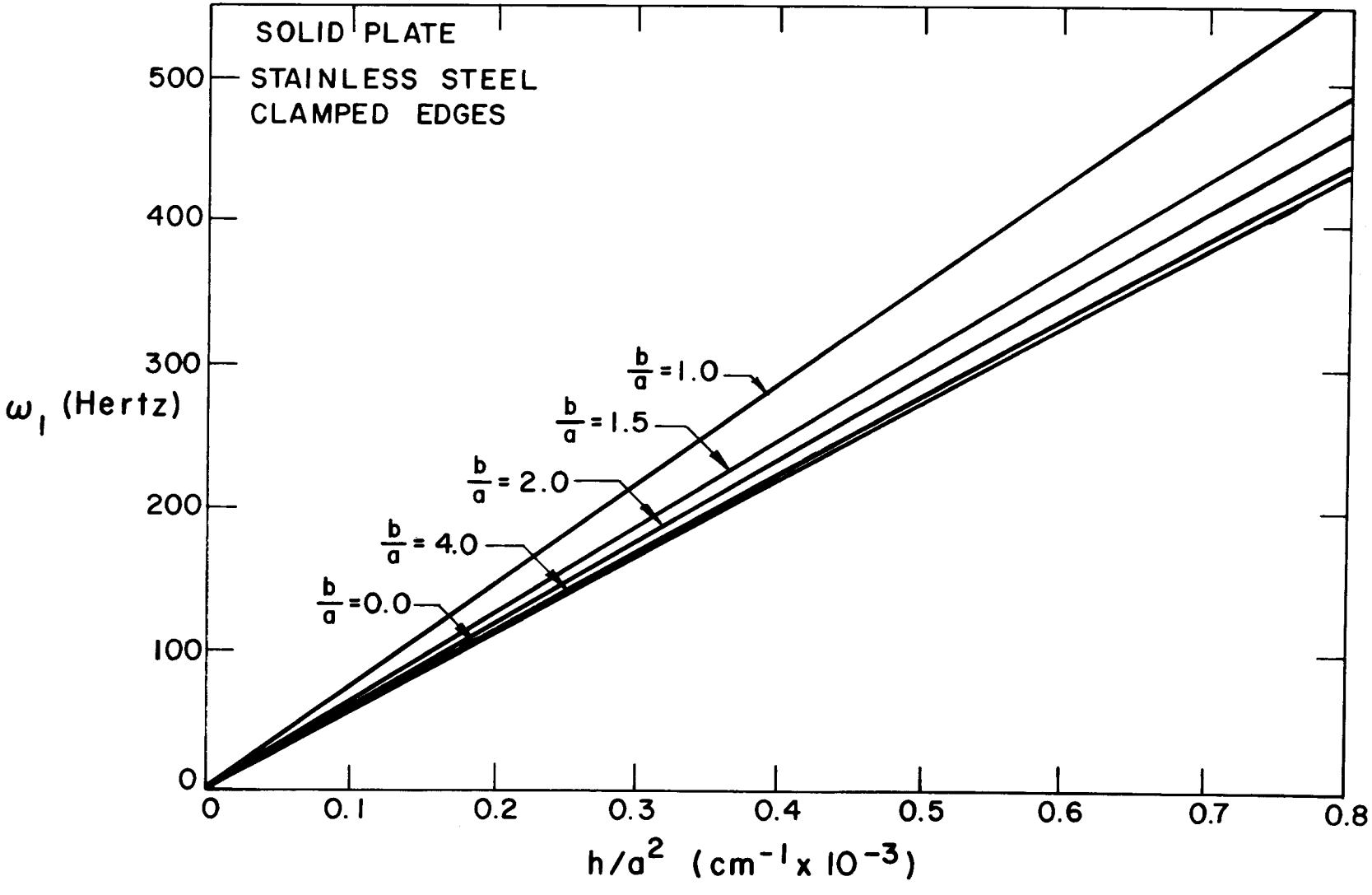

FIGURE 14

FUNDAMENTAL FREQUENCY AS A FUNCTION OF PLATE GEOMETRY

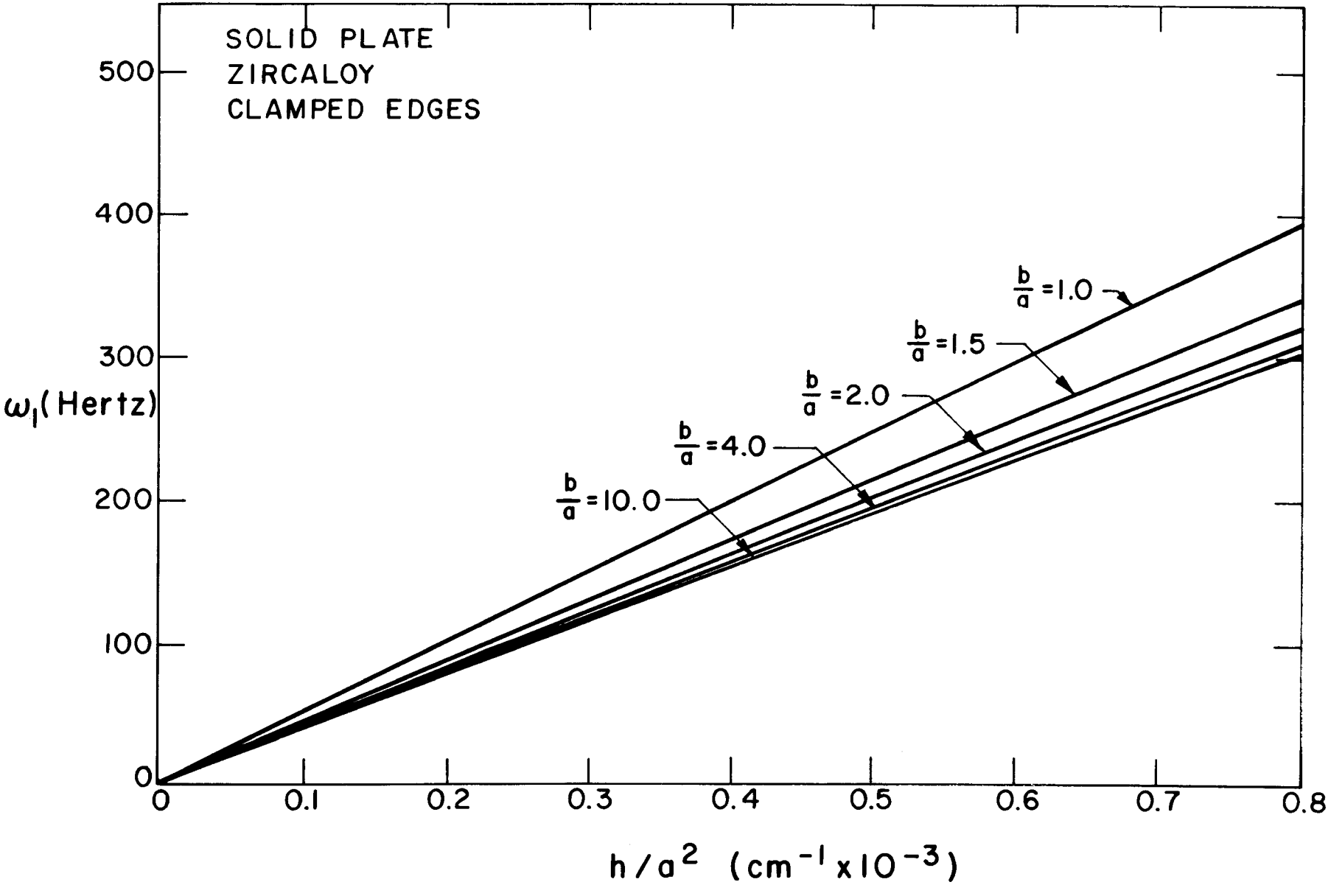

FIGURE 15

FUNDAMENTAL FREQUENCY AS A FUNCTION OF PLATE GEOMETRY

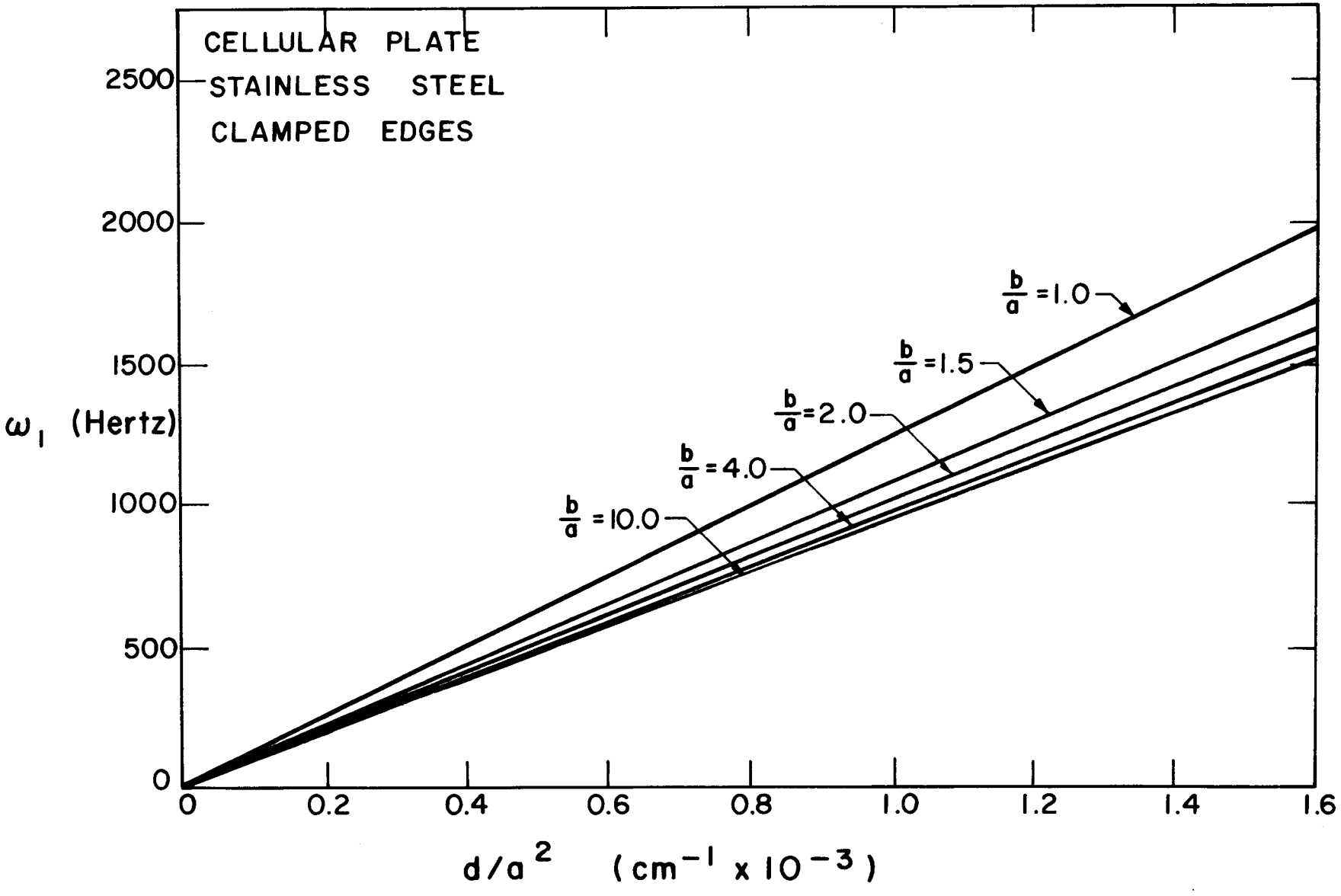

FIGURE 16

FUNDAMENTAL FREQUENCY AS A FUNCTION OF PLATE GEOMETRY

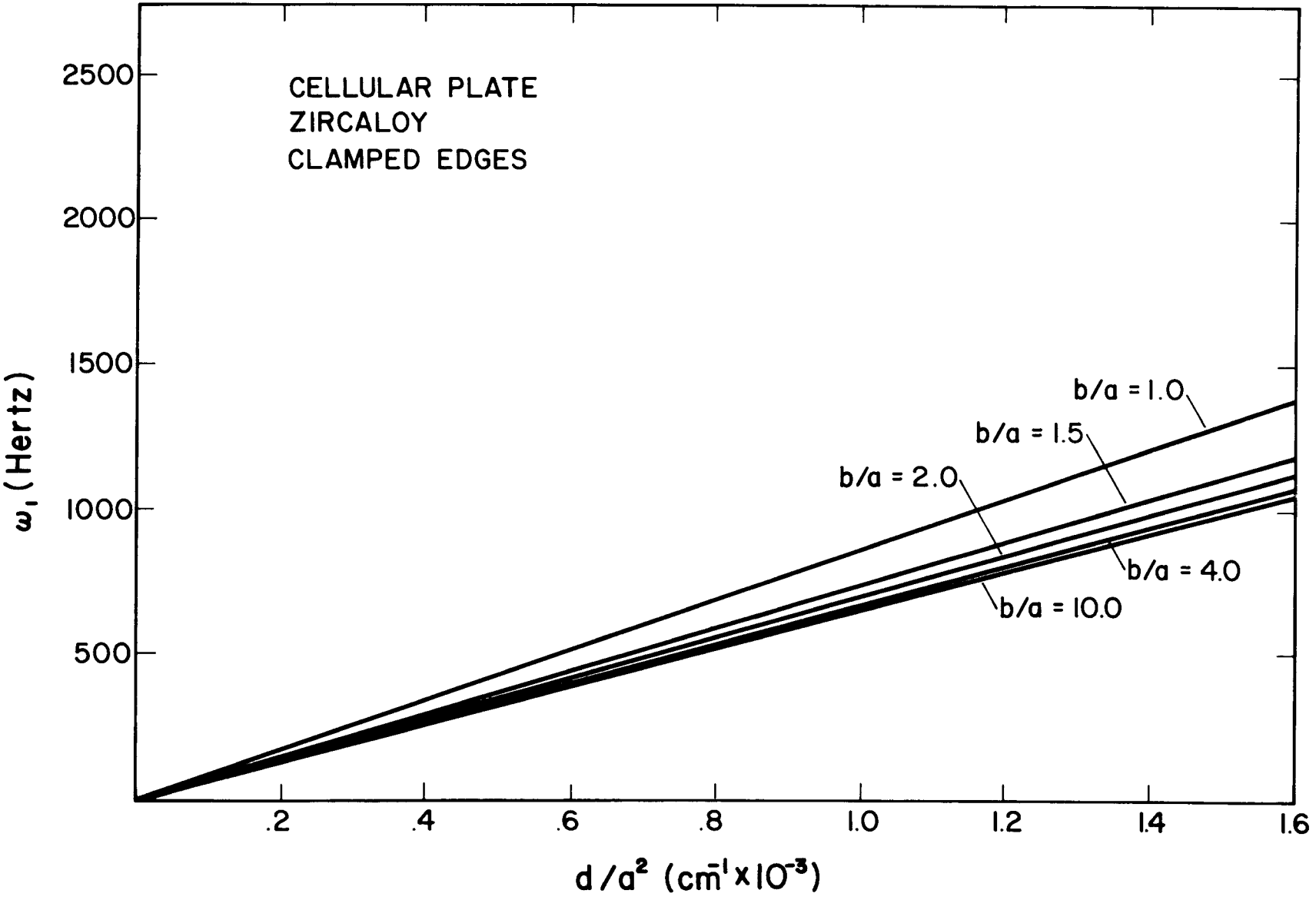

FIGURE 17

MAXIMUM DYNAMIC DEFLECTION AS A FUNCTION OF PLATE GEOMETRY

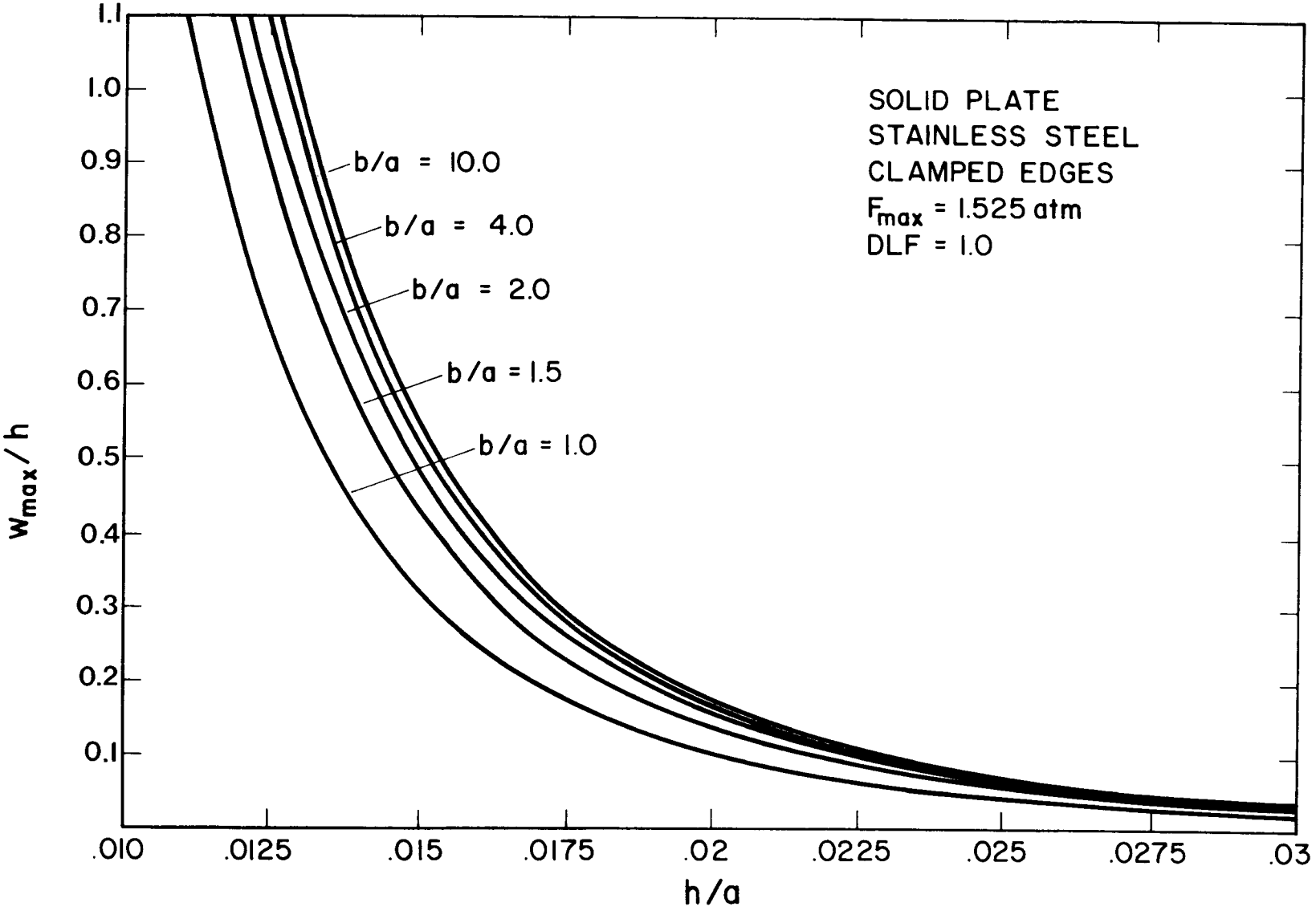

FIGURE 18

MAXIMUM DYNAMIC DEFLECTION AS A FUNCTION OF PLATE GEOMETRY

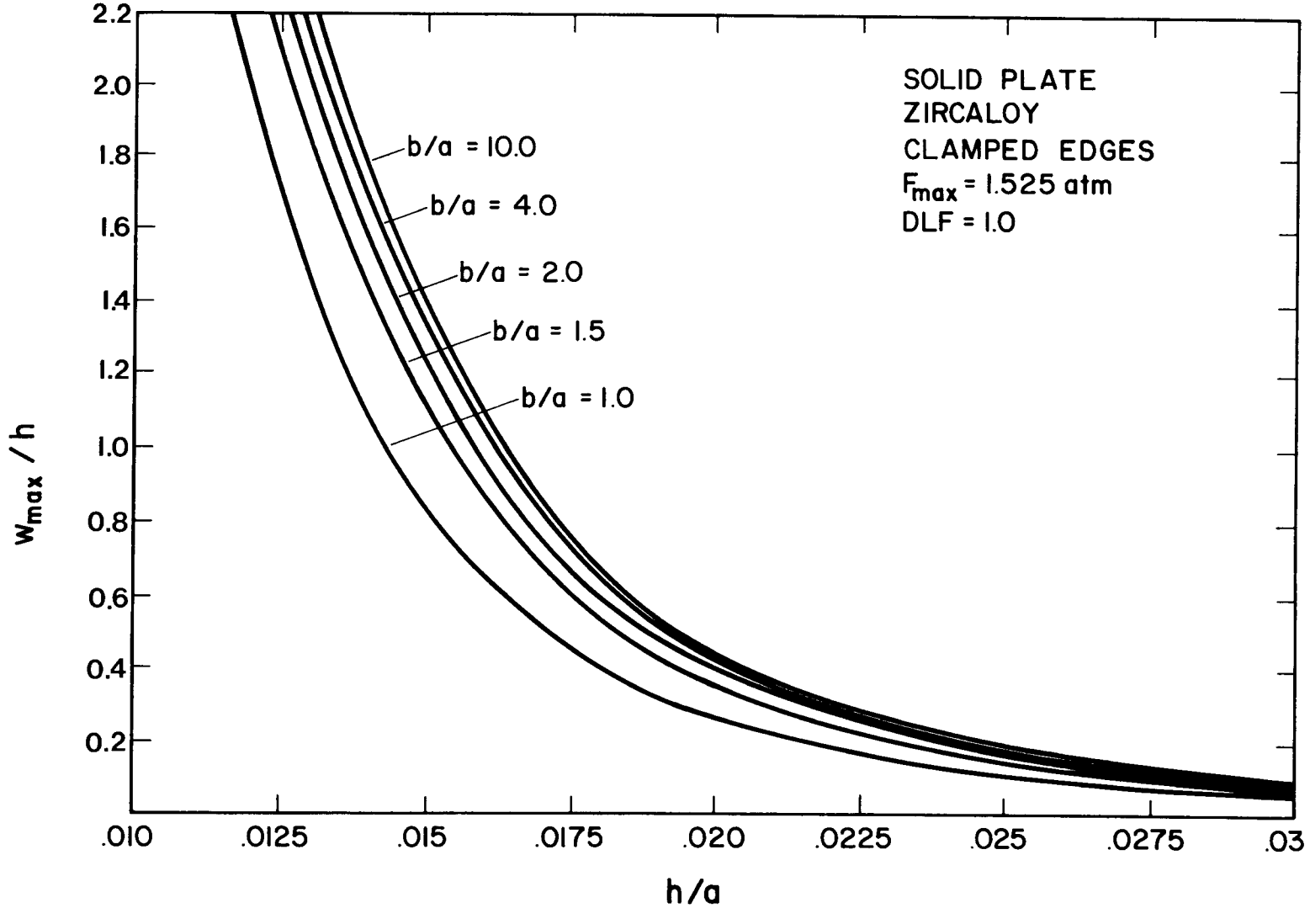

FIGURE 19

MAXIMUM DYNAMIC DEFLECTION AS A FUNCTION OF PLATE GEOMETRY

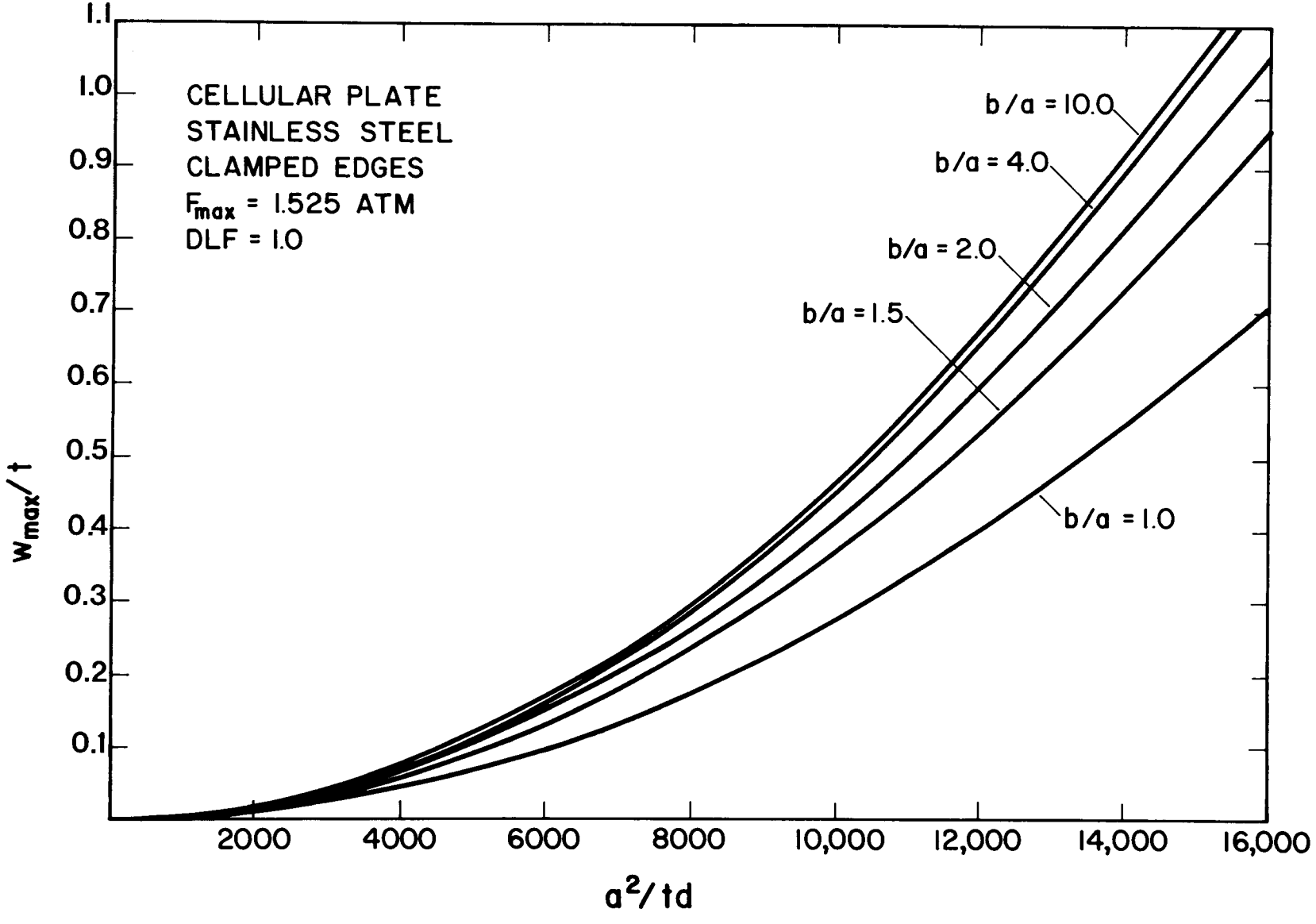

FIGURE 20

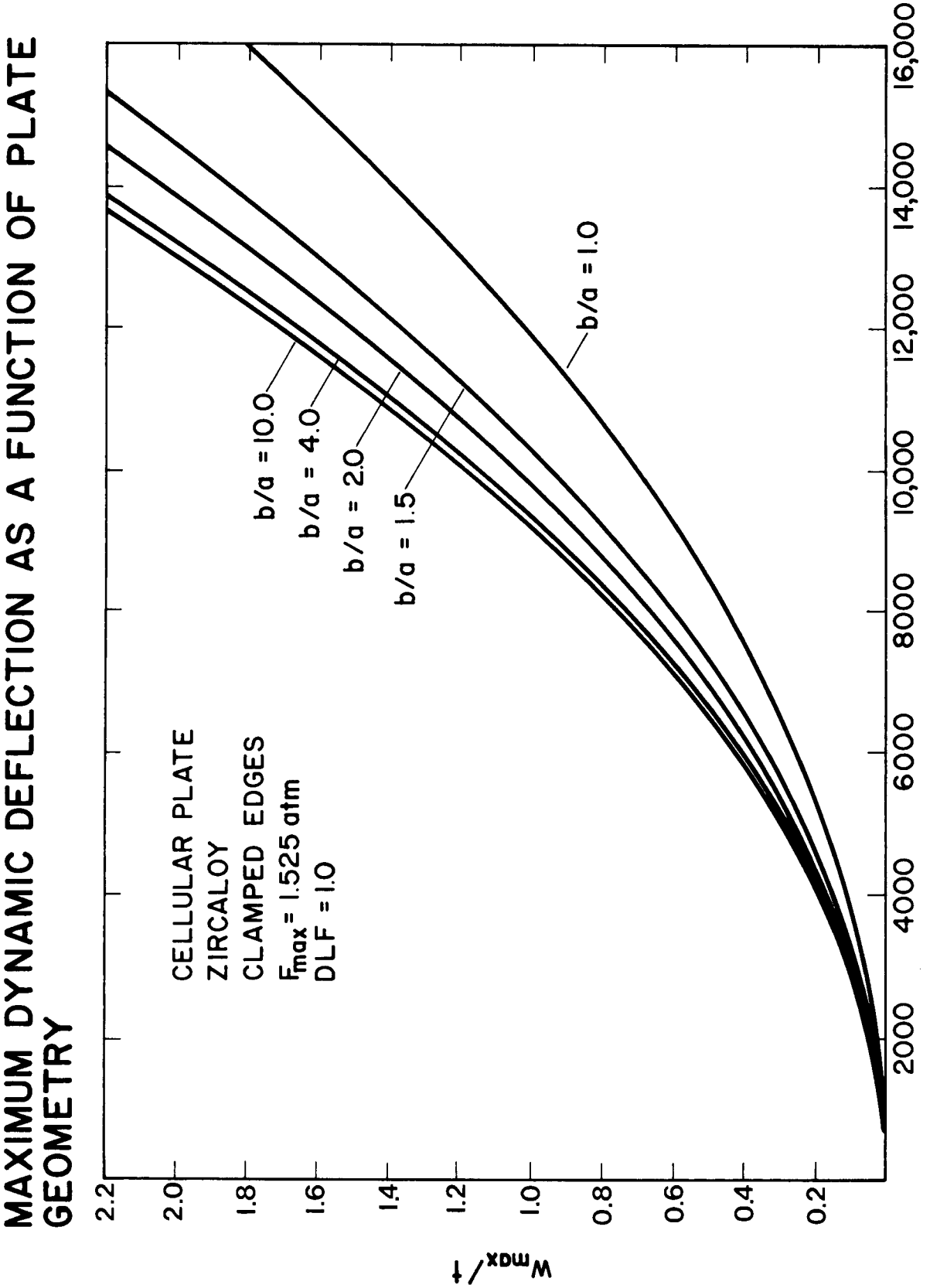
MAXIMUM DYNAMIC DEFLECTION AS A FUNCTION OF PLATE GEOMETRY
CELLULAR PLATE
ZIRCALOY
CLAMPED EDGES
F_{max} = 1.525 atm
DLF = 1.0
b/a = 10.0
b/a = 4.0
b/a = 2.0
b/a = 1.5
b/a = 1.0
W_{max}/t
a^2/td
2.2
2.0
1.8
1.6
1.4
1.2
1.0
0.8
0.6
0.4
0.2
2000
4000
6000
8000
10,000
12,000
14,000
16,000

FIGURE 21

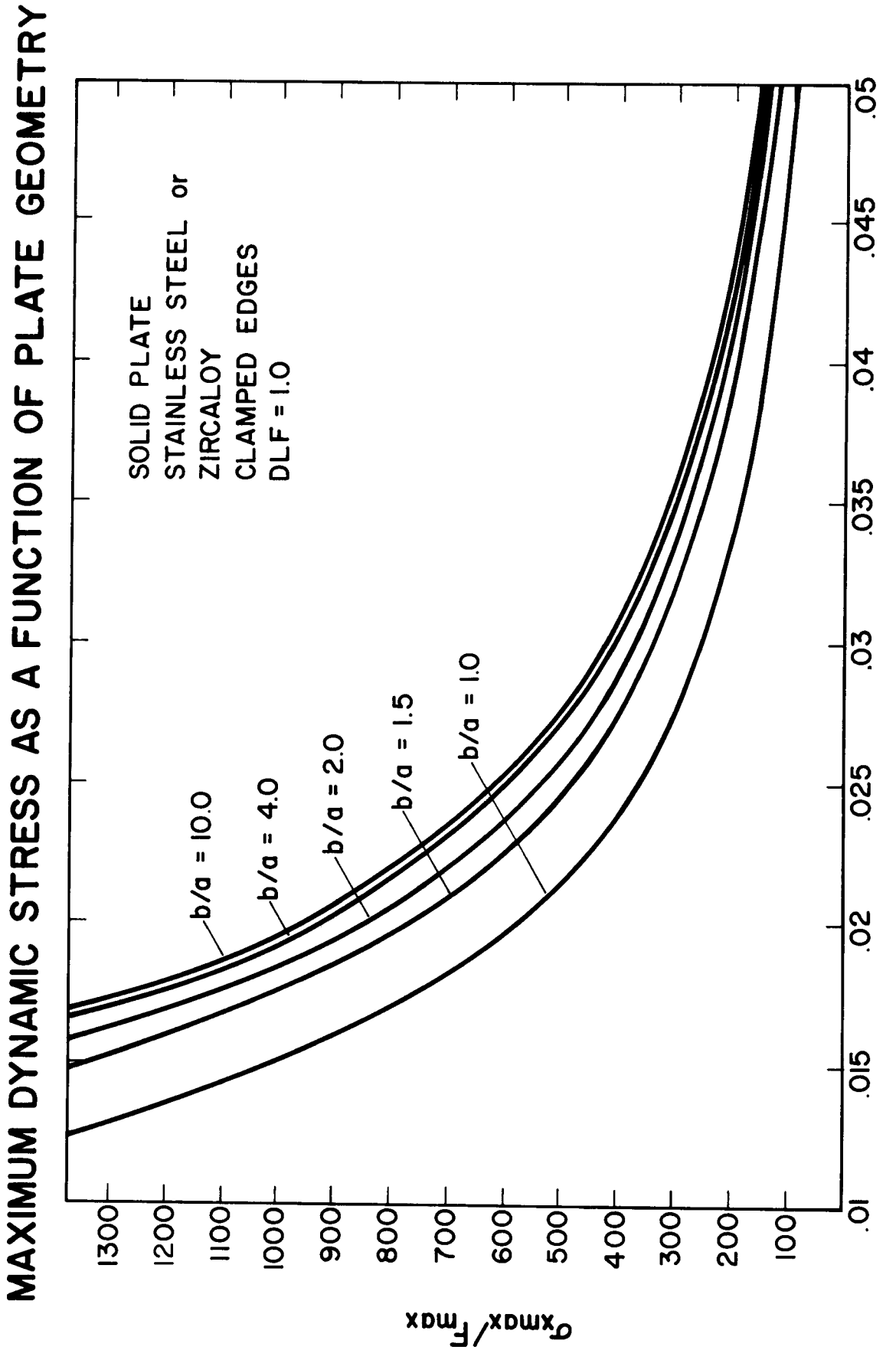
MAXIMUM DYNAMIC STRESS AS A FUNCTION OF PLATE GEOMETRY
SOLID PLATE
STAINLESS STEEL or
ZIRCALOY
CLAMPED EDGES
DLF = 1.0
b/a = 10.0
b/a = 4.0
b/a = 2.0
b/a = 1.5
b/a = 1.0
q_{xmax}/F_{max}
h/a
100
200
300
400
500
600
700
800
900
1000
1100
1200
1300
.01
.015
.02
.025
.03
.035
.04
.045
.05

FIGURE 22

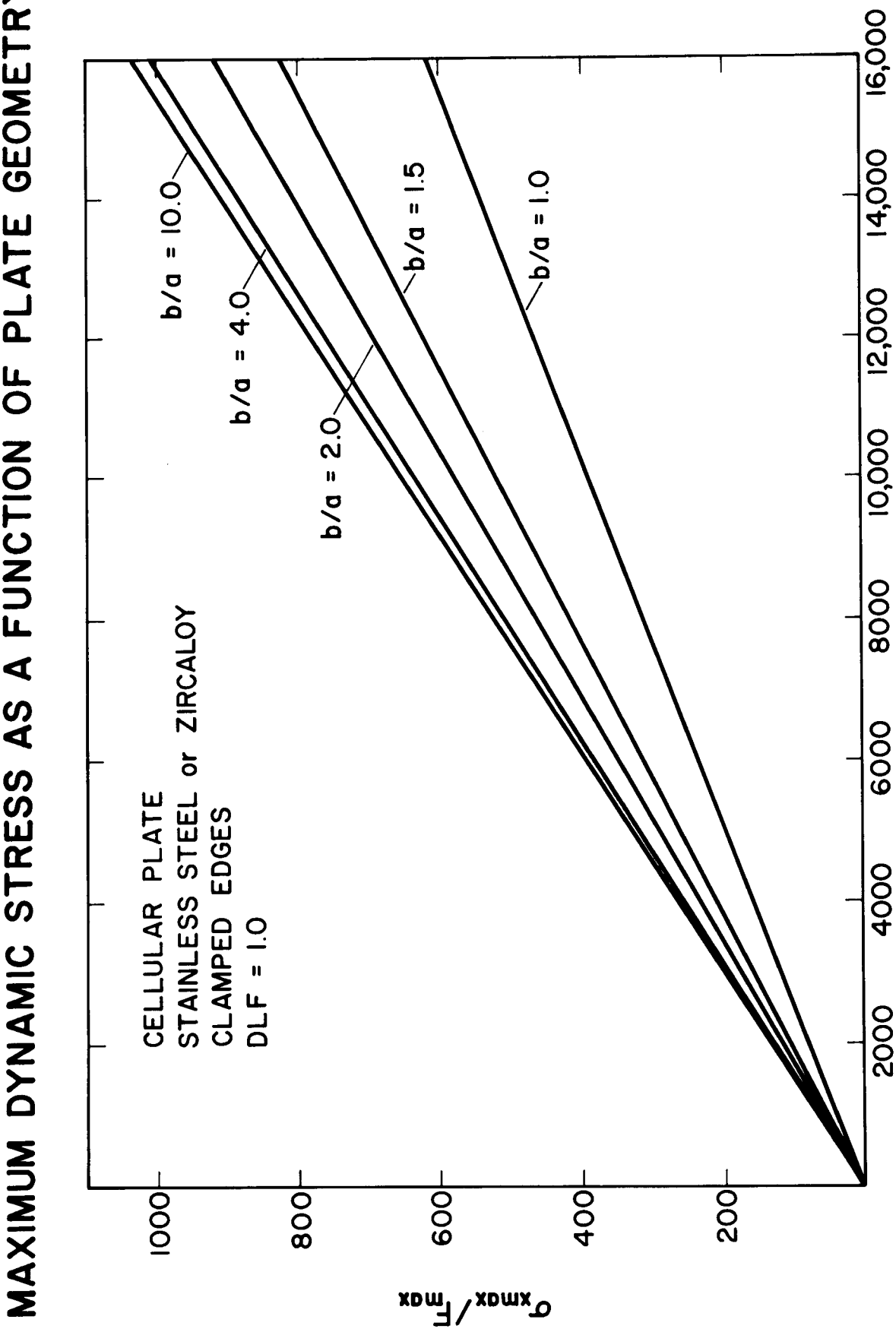
MAXIMUM DYNAMIC STRESS AS A FUNCTION OF PLATE GEOMETRY
CELLULAR PLATE
STAINLESS STEEL or ZIRCALOY
CLAMPED EDGES
DLF = 1.0
b/a = 10.0
b/a = 4.0
b/a = 2.0
b/a = 1.5
b/a = 1.0
q_{xmax}/T_{max}
d^2/td
200
400
600
800
1000
2000
4000
6000
8000
10,000
12,000
14,000
16,000

FIGURE 23

FUNDAMENTAL FREQUENCY AS A FUNCTION OF PLATE GEOMETRY

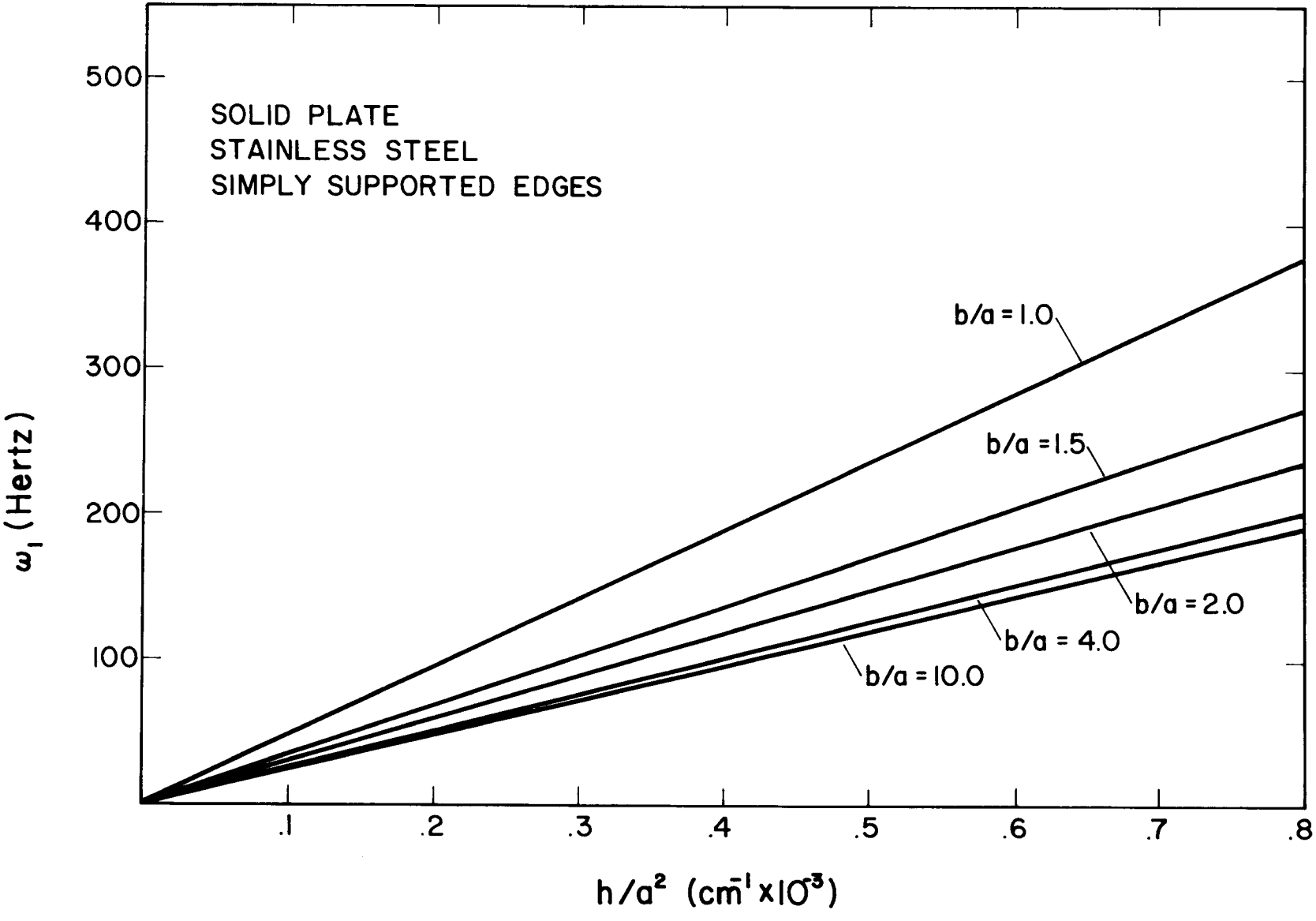

FIGURE 24

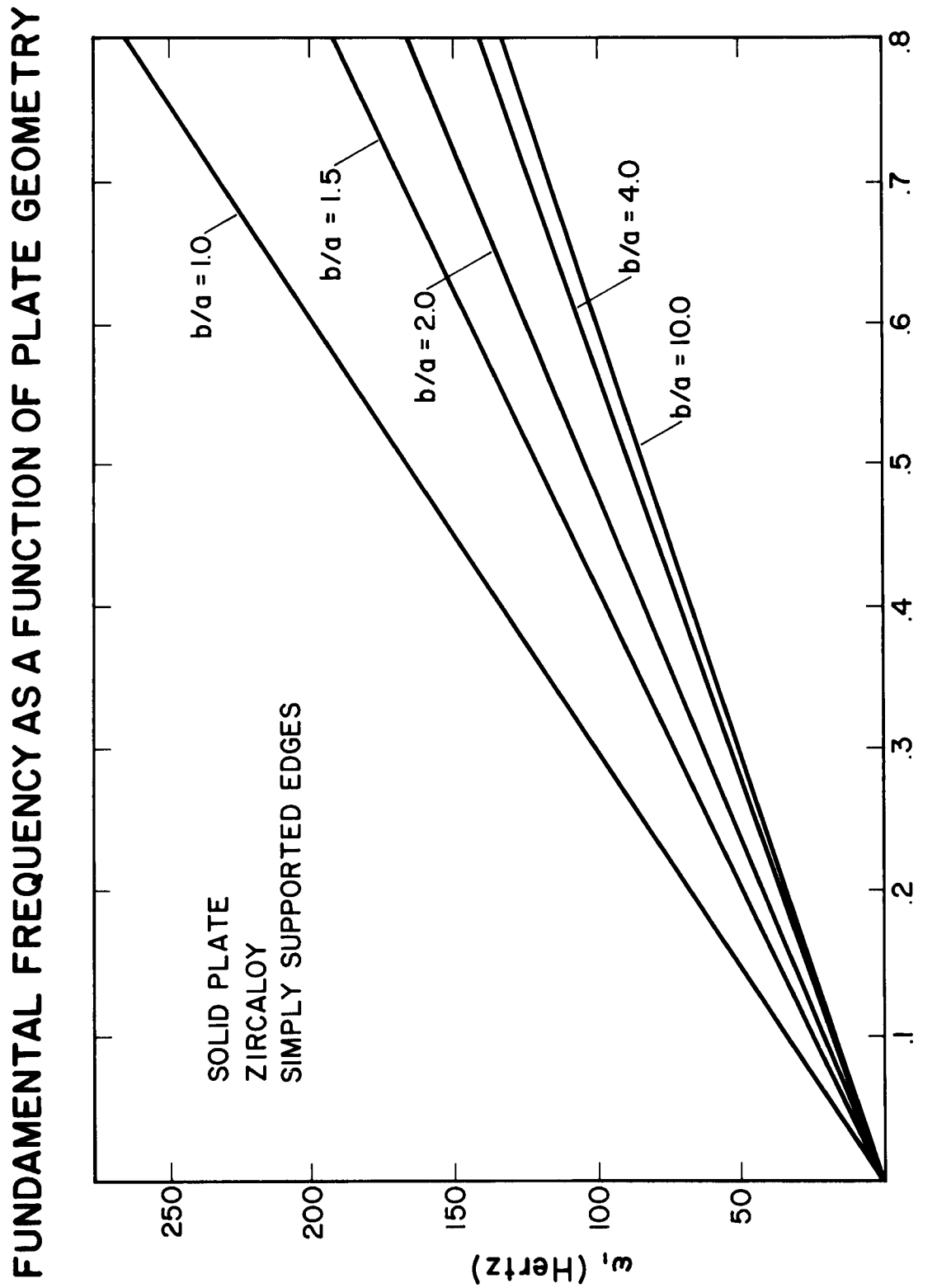
FUNDAMENTAL FREQUENCY AS A FUNCTION OF PLATE GEOMETRY
SOLID PLATE
ZIRCALOY
SIMPLY SUPPORTED EDGES
b/a = 1.0
b/a = 1.5
b/a = 2.0
b/a = 4.0
b/a = 10.0
ω1 (Hertz)
250
200
150
100
50
.1
.2
.3
.4
.5
.6
.7
.8
h/a² (cm⁻¹x10⁻³)

FIGURE 25

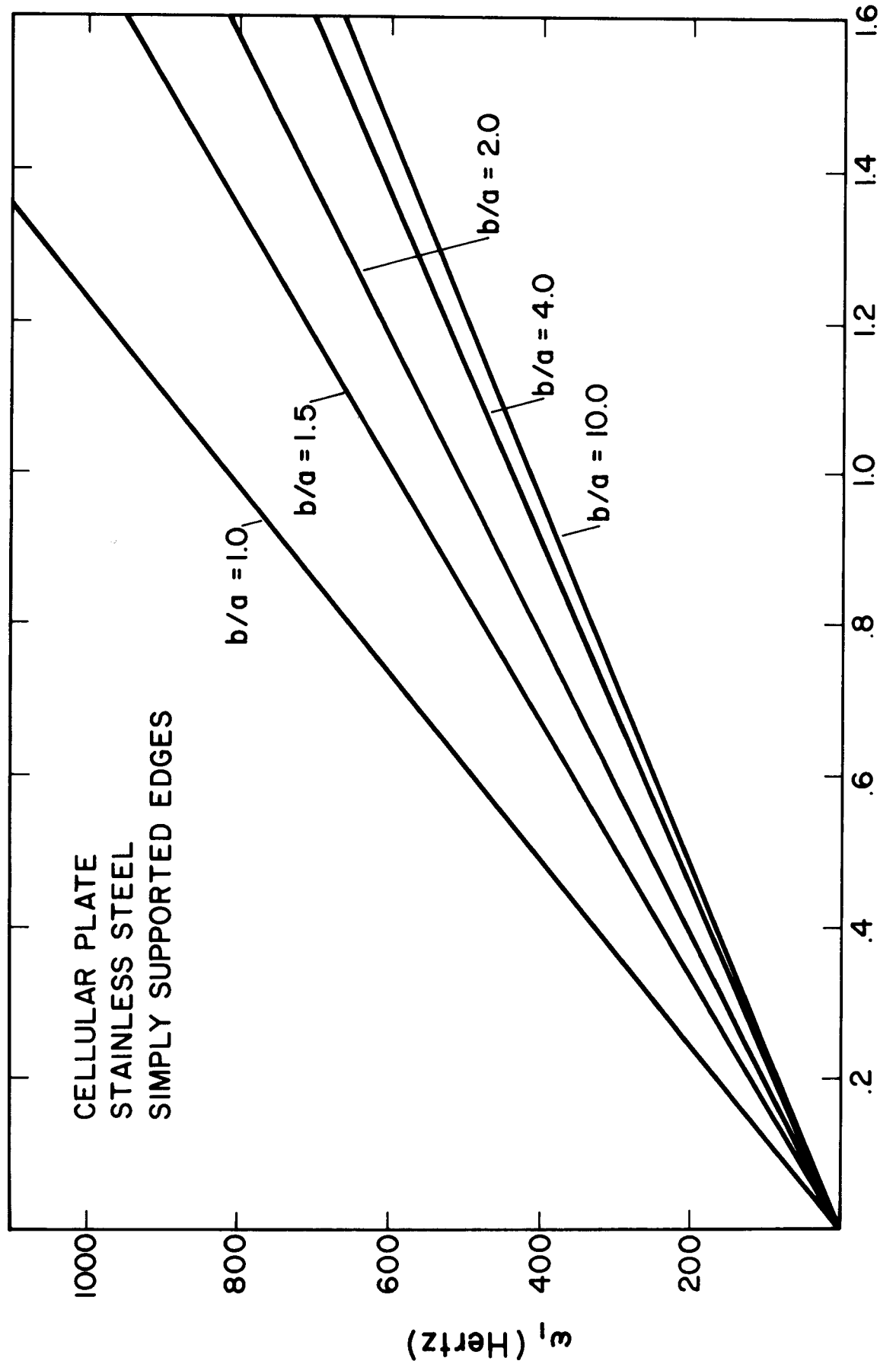
FUNDAMENTAL FREQUENCY AS A FUNCTION OF PLATE GEOMETRY
CELLULAR PLATE
STAINLESS STEEL
SIMPLY SUPPORTED EDGES
b/a = 1.0
b/a = 1.5
b/a = 2.0
b/a = 4.0
b/a = 10.0
ω_1 (Hertz)
200
400
600
800
1000
.2
.4
.6
.8
1.0
1.2
1.4
1.6
d/a^2 ($cm^{-1} \times 10^{-3}$)

FIGURE 26

FUNDAMENTAL FREQUENCY AS A FUNCTION OF PLATE GEOMETRY

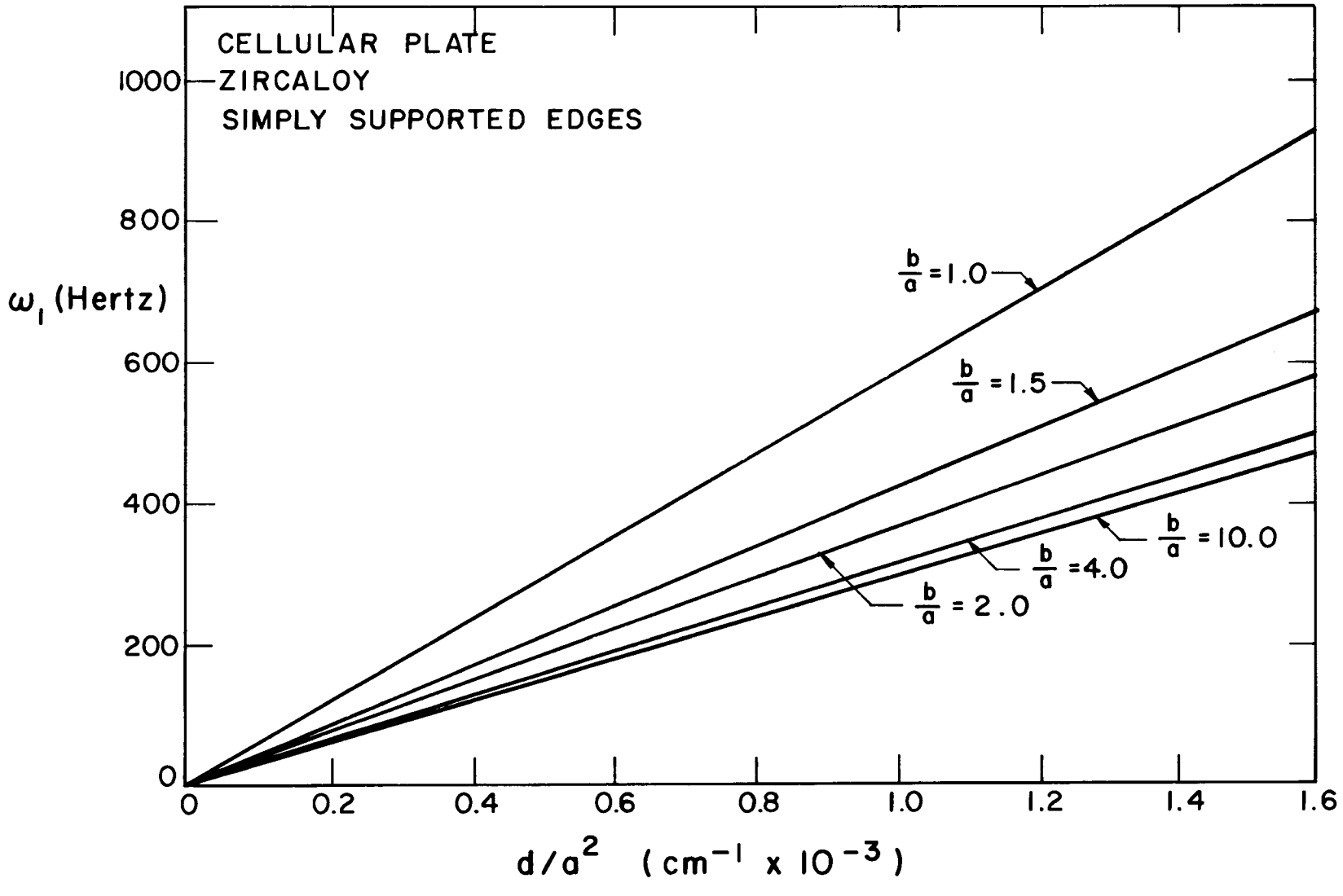

FIGURE 27

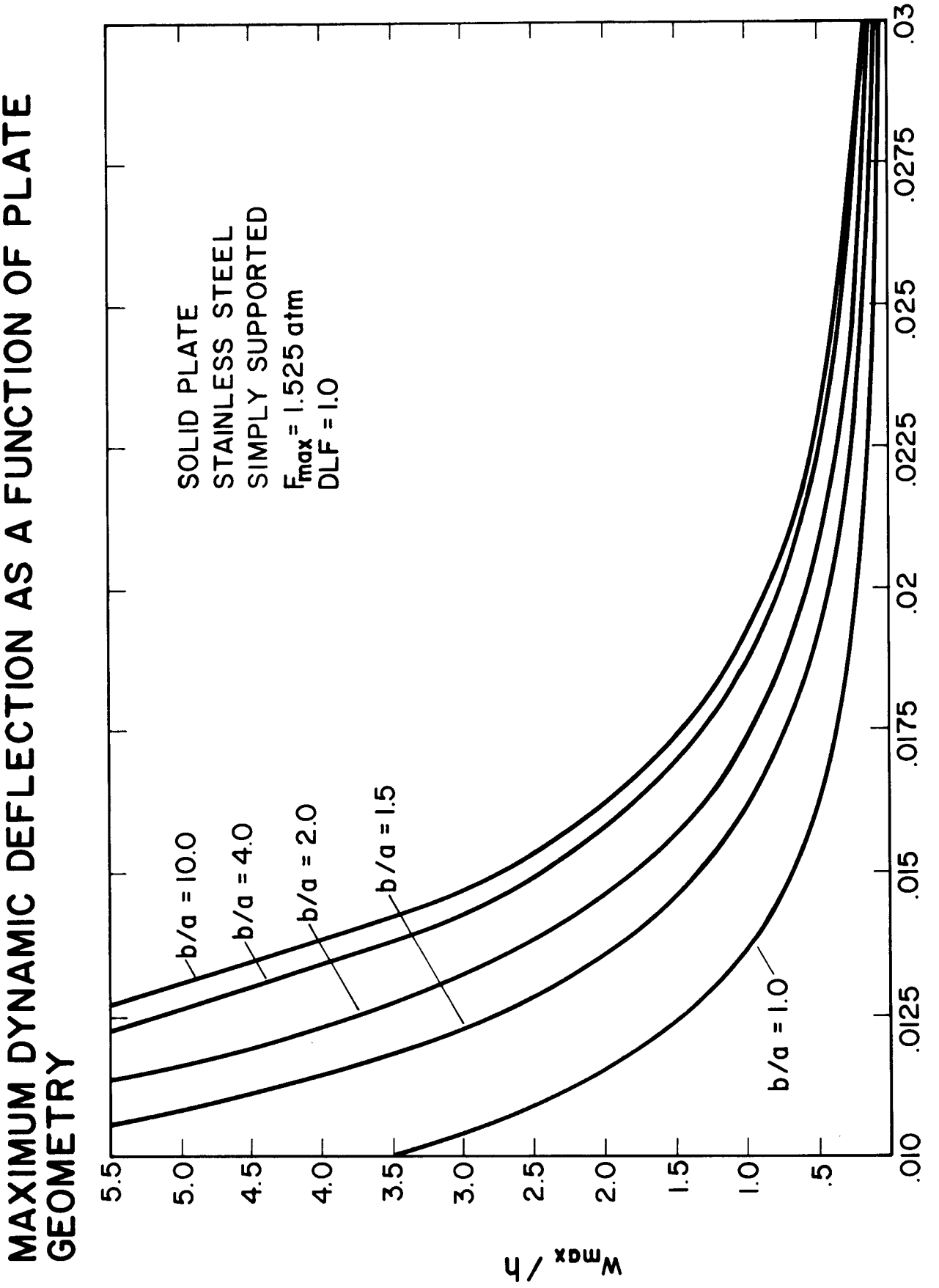
MAXIMUM DYNAMIC DEFLECTION AS A FUNCTION OF PLATE GEOMETRY
SOLID PLATE
STAINLESS STEEL
SIMPLY SUPPORTED
F_{max} = 1.525 atm
DLF = 1.0
b/a = 10.0
b/a = 4.0
b/a = 2.0
b/a = 1.5
b/a = 1.0
W_{max}/h
h/a
5.5
5.0
4.5
4.0
3.5
3.0
2.5
2.0
1.5
1.0
.5
.010
.0125
.015
.0175
.02
.0225
.025
.0275
.03

FIGURE 28

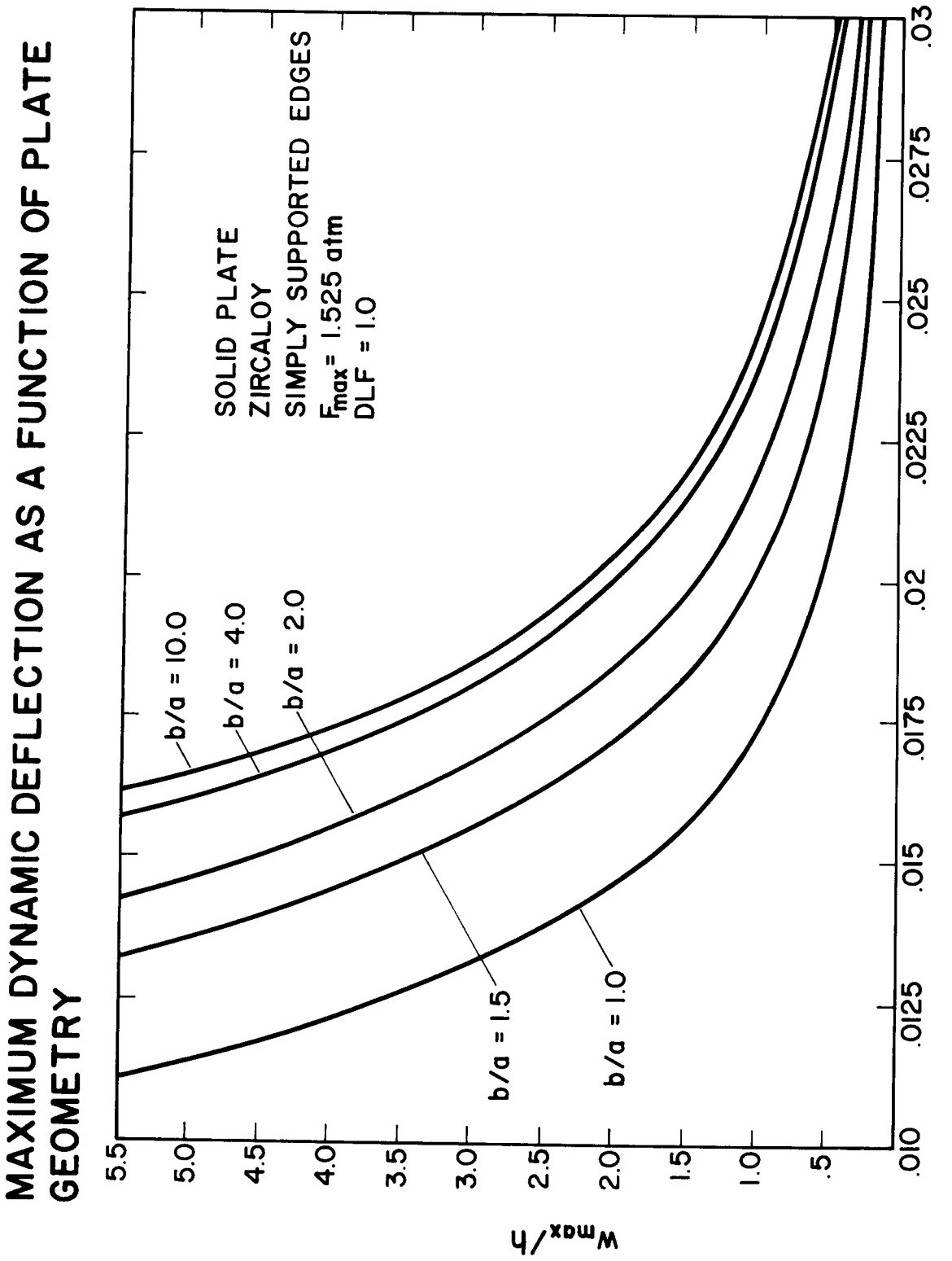
MAXIMUM DYNAMIC DEFLECTION AS A FUNCTION OF PLATE GEOMETRY
SOLID PLATE
ZIRCALOY
SIMPLY SUPPORTED EDGES
F_{max}= 1.525 atm
DLF = 1.0
b/a = 10.0
b/a = 4.0
b/a = 2.0
b/a = 1.5
b/a = 1.0
W_{max}/h
h/a
5.5
5.0
4.5
4.0
3.5
3.0
2.5
2.0
1.5
1.0
.5
.010
.0125
.015
.0175
.02
.0225
.025
.0275
.03

FIGURE 29

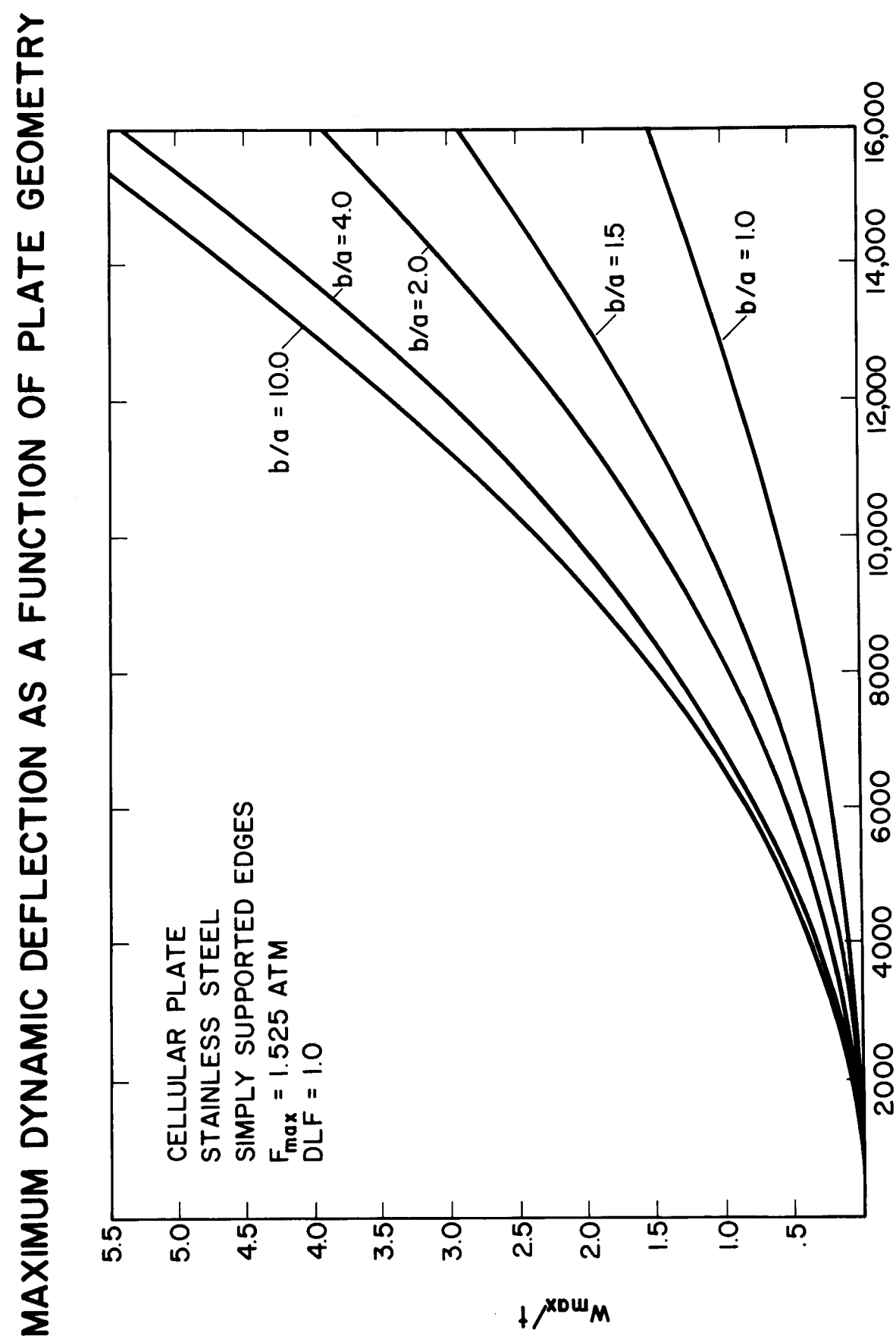
MAXIMUM DYNAMIC DEFLECTION AS A FUNCTION OF PLATE GEOMETRY
CELLULAR PLATE
STAINLESS STEEL
SIMPLY SUPPORTED EDGES
F_{max} = 1.525 ATM
DLF = 1.0
b/a = 10.0
b/a = 4.0
b/a = 2.0
b/a = 1.5
b/a = 1.0
W_{max}/t
a^2/td
5.5
5.0
4.5
4.0
3.5
3.0
2.5
2.0
1.5
1.0
.5
2000
4000
6000
8000
10,000
12,000
14,000
16,000

FIGURE 30

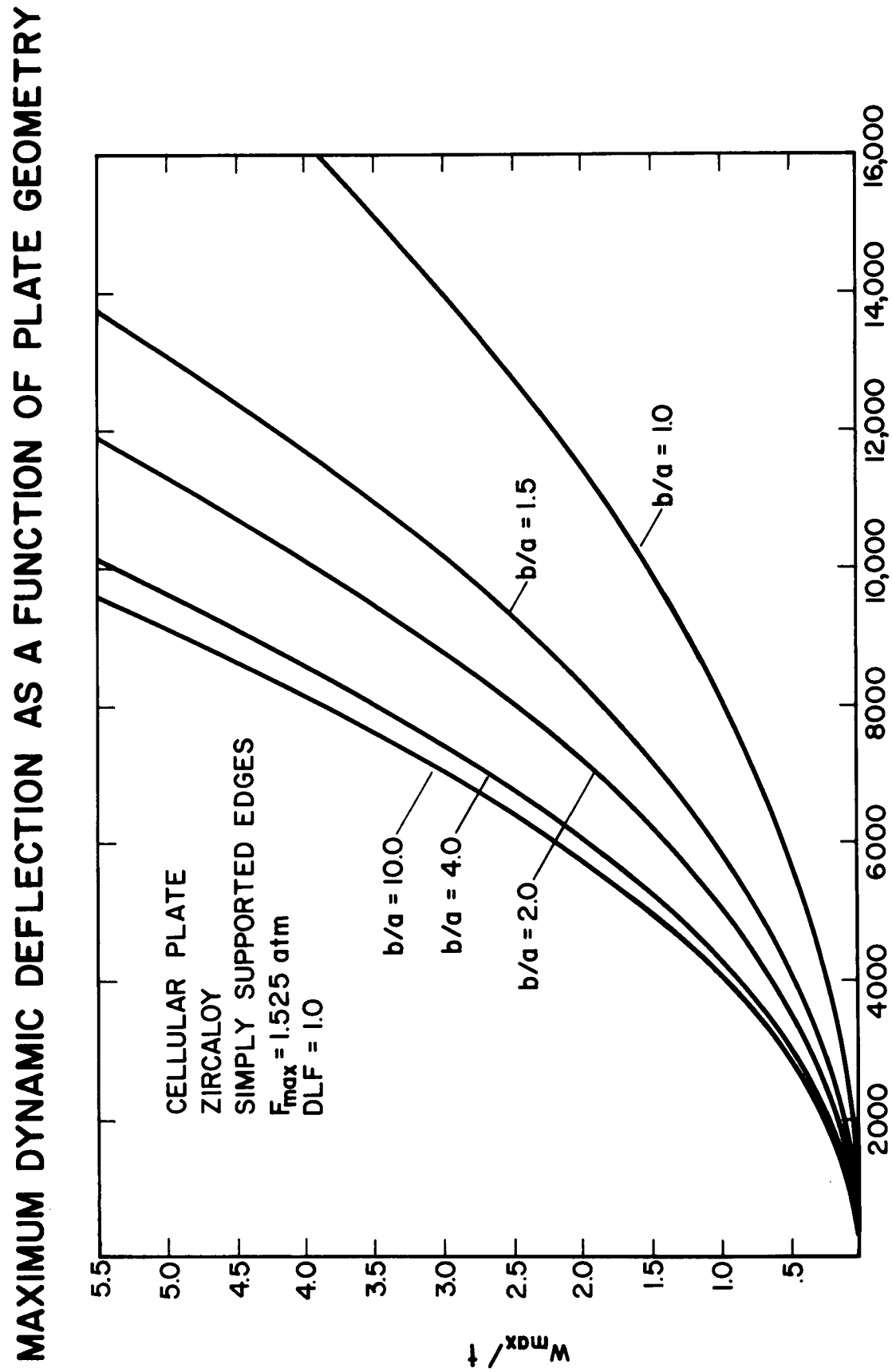
MAXIMUM DYNAMIC DEFLECTION AS A FUNCTION OF PLATE GEOMETRY
CELLULAR PLATE
ZIRCALOY
SIMPLY SUPPORTED EDGES
F_{max} = 1.525 atm
DLF = 1.0
b/a = 10.0
b/a = 4.0
b/a = 2.0
b/a = 1.5
b/a = 1.0
W_{max}/t
a^2/td
5.5
5.0
4.5
4.0
3.5
3.0
2.5
2.0
1.5
1.0
.5
2000
4000
6000
8000
10,000
12,000
14,000
16,000

FIGURE 31

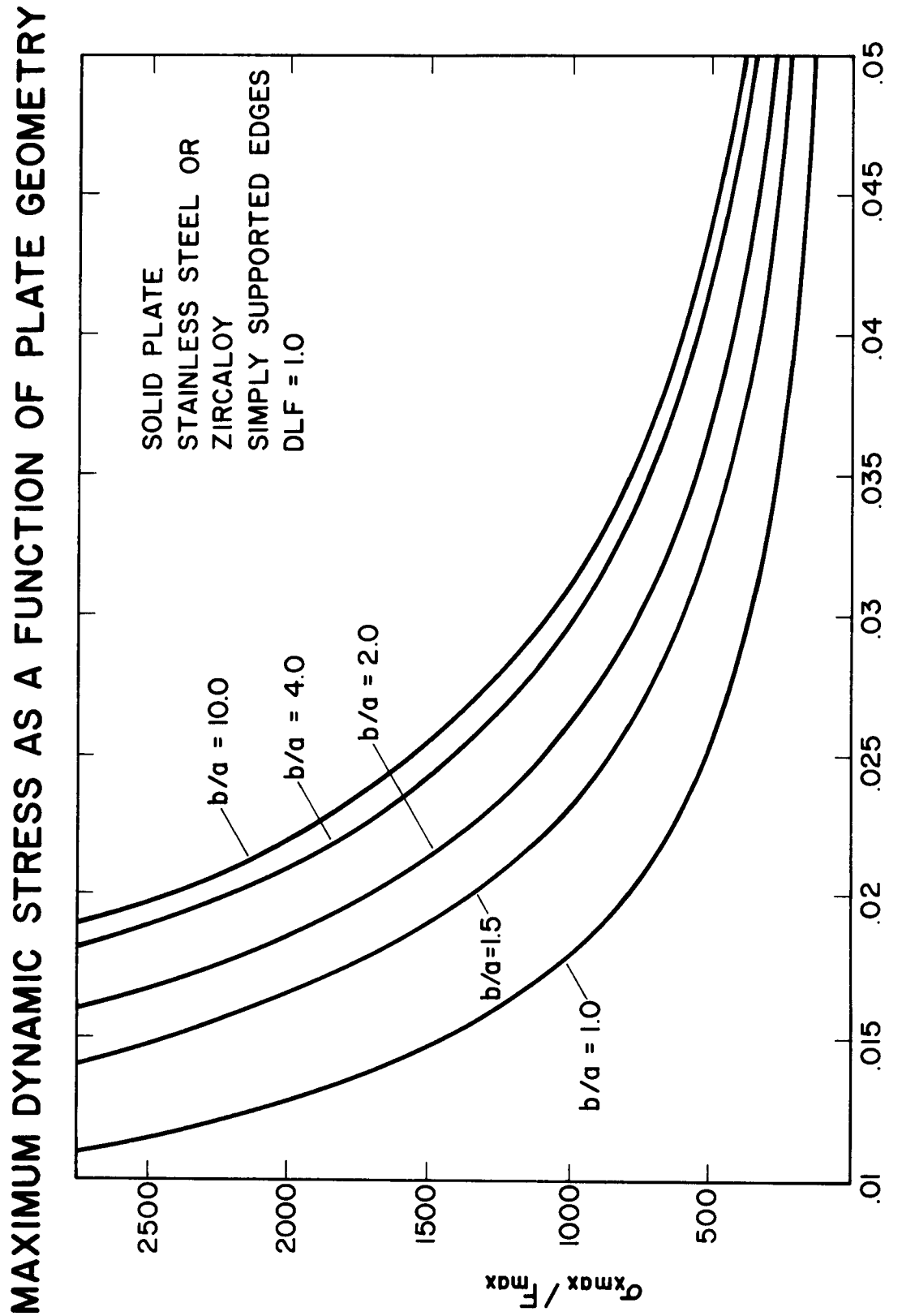
MAXIMUM DYNAMIC STRESS AS A FUNCTION OF PLATE GEOMETRY
SOLID PLATE
STAINLESS STEEL OR
ZIRCALOY
SIMPLY SUPPORTED EDGES
DLF = 1.0
b/a = 10.0
b/a = 4.0
b/a = 2.0
b/a=1.5
b/a = 1.0
q_{xmax} / T_{max}
2500
2000
1500
1000
500
.01
.015
.02
.025
.03
.035
.04
.045
.05
h/a

FIGURE 32

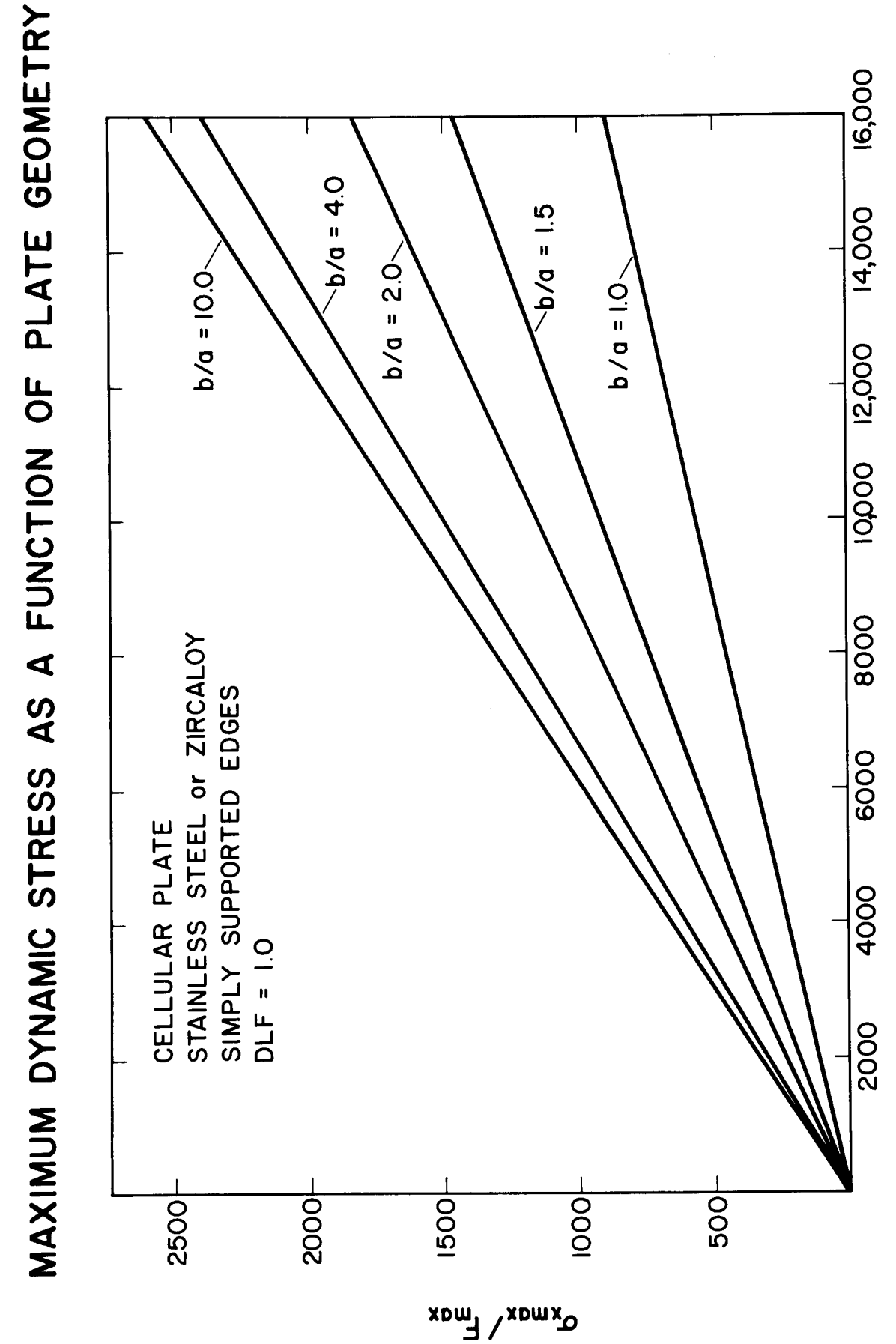
MAXIMUM DYNAMIC STRESS AS A FUNCTION OF PLATE GEOMETRY
CELLULAR PLATE
STAINLESS STEEL or ZIRCALOY
SIMPLY SUPPORTED EDGES
DLF = 1.0
b/a = 10.0
b/a = 4.0
b/a = 2.0
b/a = 1.5
b/a = 1.0
q_{xmax}/π_{max}
a^2/td
500
1000
1500
2000
2500
2000
4000
6000
8000
10,000
12,000
14,000
16,000

FIGURE 33

Procedure for Designing a Solid Plate

1. Choose a value for the thickness h and the plate dimensions a and b.
2. Calculate b/a, h/a, and h/a^2.
3. From the appropriate frequency curve determine a value for the fundamental frequency ω_1.
4. For this frequency determine the corresponding maximum DLF from Figure 13.
5. From the appropriate stress and deflection curves determine values for $\sigma_{x_{max}}/F_{max}$ and w_{max}/h.
6. To find the absolute dynamic stress, multiply $\sigma_{x_{max}}/F_{max}$ by the DLF and by the overpressure F_{max}.
7. To find the absolute dynamic deflection, multiply w_{max}/h by the DLF and by the corresponding value of h.
8. Determine if the dynamic stress and deflection are acceptable by comparing with design limits.

Procedure for Designing a Cellular Plate

1. Choose a value for the parameter d and the plate dimensions a and b.
2. Calculate b/a and d/a^2.
3. From the appropriate frequency curve determine a value for the fundamental frequency ω_1.
4. For this frequency determine the corresponding maximum DLF from Figure 13.
5. Using a maximum stress limit and an overpressure F_{max}, calculate $\sigma_{x_{max}}/F_{max}$ and divide this by the DLF.
6. From the appropriate stress curve determine a value for the plate geometry term a^2/td.
7. Knowing a and d, calculate t.
8. From the appropriate deflection curve determine a value for w_{max}/t.
9. To find the absolute dynamic deflection multiply w_{max}/t by the corresponding value of t.
10. Establish the viability of these answers by a comparison with design limits.

A detailed example has been developed to compare the dynamic response of solid clamped stainless steel and zircaloy plates. Calculations are also included for a clamped stainless steel cellular plate to illustrate the added stiffness of such a structure. Design parameters used are given in Table 2. Input parameters for a solid plate (stainless steel or zircaloy) are included in Table 3. Using the design procedure previously outlined, results for the stainless steel and zircaloy plates are shown in Tables 4 and 5 respectively. For a cellular plate, input parameters are given in Table 6, with design curve results shown in Table 7.

TABLE 2

Design Parameters

Shell Radius	= 400 cm
Circumference	= 2513.27 cm
Gas Duct Radius	= 170 cm
Plate Height b	= 420 cm
Maximum Working Stress σ_w	= 20 ksi (used with cellular plate)
Maximum Overpressure F_{max}	= 22.42 psi

TABLE 3

Input Parameters for Solid Stainless Steel or Zircaloy Plates

Case	No. of Panels	a(cm)	b/a	h(cm)	h/a	$h/a^2(cm^{-1}x10^{-3})$
(1)	16	157.08	2.67	1.0	0.00637	0.0405
(2)	24	104.72	4.01	1.0	0.00955	0.0912
(3)	32	78.54	5.35	1.0	0.01273	0.1621
(4)	40	62.83	6.68	1.0	0.01592	0.2533
(5)	48	52.36	8.02	1.0	0.01910	0.3647
(6)	56	44.88	9.36	1.0	0.02228	0.4965
(7)	16	157.08	2.67	1.5	0.00955	0.0608
(8)	24	104.72	4.01	1.5	0.01432	0.1368
(9)	32	78.54	5.35	1.5	0.01910	0.2432
(10)	40	62.83	6.68	1.5	0.02387	0.3800
(11)	48	52.36	8.02	1.5	0.02865	0.5471
(12)	56	44.88	9.36	1.5	0.03342	0.7447
(13)	16	157.08	2.67	2.0	0.01273	0.0811
(14)	24	104.72	4.01	2.0	0.01910	0.1824
(15)	32	78.54	5.35	2.0	0.02546	0.3242
(16)	40	62.83	6.68	2.0	0.03183	0.5066
(17)	48	52.36	8.02	2.0	0.03820	0.7295
(18)	56	44.88	9.36	2.0	0.04456	0.9929
(19)	16	157.08	2.67	2.5	0.01592	0.1010
(20)	24	104.72	4.01	2.5	0.02387	0.2280
(21)	32	78.54	5.35	2.5	0.03183	0.4053
(22)	40	62.83	6.68	2.5	0.03979	0.6333
(23)	48	52.36	8.02	2.5	0.04775	0.9119
(24)	56	44.88	9.36	2.5	0.05570	1.2412

TABLE 4

Design Curve Results for a Solid Stainless Steel Plate with Clamped Edges

Case	ω_1(Hz)	DLF_{max}	$\sigma_{x_{max}}/F_{max}$	w_{max}/h	σ_x(ksi)	w(cm)
(1)	23	1.00	>1400	>1.000	>20.0	>1.000
(2)	50	1.00	>1400	>1.000	>20.0	>1.000
(3)	90	1.00	>1400	1.060	>20.0	1.060
(4)	140	1.00	>1400	0.430	>20.0	0.430
(5)	200	1.20	1060	0.208	28.5	0.250
(6)	270	1.36	775	0.112	23.6	0.152
(7)	34	1.00	>1400	>1.000	>20.0	>1.000
(8)	76	1.00	>1400	0.644	>20.0	0.966
(9)	134	1.00	1040	0.210	23.3	0.315
(10)	210	1.24	670	0.086	18.6	0.160
(11)	300	1.41	470	0.040	14.9	0.085
(12)	406	1.53	345	<0.030	11.8	<0.080
(13)	46	1.00	>1400	1.000	>20.0	2.000
(14)	100	1.00	1025	0.204	23.0	0.408
(15)	180	1.12	590	0.060	14.8	0.134
(16)	277	1.37	380	0.028*	11.7	0.077
(17)	400	1.53	260	<0.030	8.9	<0.080
(18)	542*	1.64	195	<0.030	7.2	<0.080
(19)	57	1.00	1420*	0.400	31.8	1.000
(20)	126	1.00	660	0.084	14.8	0.210
(21)	220	1.26	380	0.028*	10.7	0.088
(22)	347	1.47	240	<0.030	7.9	<0.080
(23)	500	1.61	165	<0.030	6.0	<0.080
(24)	677*	1.70	125*	<0.030	4.8	<0.080

*Extrapolated

TABLE 5

Design Curve Results for a Solid Zircaloy Plate with Clamped Edges

Case	ω_1(Hz)	DLF_{max}	$\sigma_{x_{max}}/F_{max}$	w_{max}/h	σ_x(ksi)	w(cm)
(1)	16	1.00	>1400	>2.000	>20.0	>2.000
(2)	35	1.00	>1400	>2.000	>20.0	>2.000
(3)	62	1.00	>1400	>2.000	>20.0	>2.000
(4)	97	1.00	>1400	1.100	>20.0	1.100
(5)	139	1.00	1060	0.530	23.8	0.530
(6)	190	1.18	775	0.290	20.5	0.342
(7)	24	1.00	>1400	>2.000	>20.0	>2.000
(8)	53	1.00	>1400	1.640	>20.0	2.460
(9)	93	1.00	1040	0.520	23.3	0.780
(10)	146	1.00	670	0.220	15.0	0.330
(11)	209	1.22	470	0.100	12.9	0.183
(12)	284	1.38	345	<0.100	10.7	<0.200
(13)	32	1.00	>1400	>2.000	>20.0	>2.000
(14)	71	1.00	1025	0.520	23.0	1.040
(15)	125	1.00	590	0.164	13.2	0.328
(16)	194	1.20	380	<0.100	10.2	<0.200
(17)	279	1.37	260	<0.100	8.0	<0.200
(18)	379	1.50	195	<0.100	6.6	<0.200
(19)	40	1.00	1420*	1.040	31.8	2.600
(20)	86	1.00	660	0.220	15.8	0.550
(21)	156	1.10	380	0.070	9.4	0.193
(22)	243	1.31	240	<0.100	7.0	<0.200
(23)	349	1.47	165	<0.100	5.4	<0.200
(24)	474	1.59	125*	<0.100	4.5	<0.200

*Extrapolated

TABLE 6

Input Parameters for Cellular Stainless Steel or Zircaloy Plates

Case	No. of Panels	a(cm)	b/a	d(cm)	$d/a^2(cm^{-1}x10^{-3})$
(1)	8	314.16	1.34	2.0	0.0202
(2)	16	157.08	2.67	2.0	0.0811
(3)	24	104.72	4.01	2.0	0.1824
(4)	32	78.54	5.35	2.0	0.3242
(5)	40	62.83	6.68	2.0	0.5066
(6)	48	52.36	8.02	2.0	0.7295
(7)	8	314.16	1.34	3.0	0.0304
(8)	16	157.08	2.67	3.0	0.1216
(9)	24	104.72	4.01	3.0	0.2736
(10)	32	78.54	5.35	3.0	0.4863
(11)	40	62.83	6.68	3.0	0.7600
(12)	48	52.36	8.02	3.0	1.0943
(13)	8	314.16	1.34	4.0	0.0404
(14)	16	157.08	2.67	4.0	0.1621
(15)	24	104.72	4.01	4.0	0.3648
(16)	32	78.54	5.35	4.0	0.6484
(17)	40	62.83	6.68	4.0	1.0133
(18)	48	52.36	8.02	4.0	1.4590
(19)	8	314.16	1.34	5.0	0.0507
(20)	16	157.08	2.67	5.0	0.2026
(21)	24	104.72	4.01	5.0	0.4559
(22)	32	78.54	5.35	5.0	0.8106
(23)	40	62.83	6.68	5.0	1.2666
(24)	48	52.36	8.02	5.0	1.8238

TABLE 7

Design Curve Results for a Cellular Stainless Steel Plate with Clamped Edges

Case	ω_1(Hz)	DLF_{max}	892/DLF**	a^2/td	t(cm)	w_{max}/t	w(cm)
(1)	22	1.00	892	18,500*	2.676	>1.000	>1.000
(2)	80	1.00	892	14,900	0.828	0.964	0.798
(3)	182	1.12	796	12,700	0.432	0.730	0.315
(4)	308	1.42	628	9,900	0.312	0.450	0.140
(5)	480	1.60	557	8,700	0.227	0.348	0.079
(6)	690	1.71	522	8,200	0.167	0.310	0.052
(7)	33	1.00	892	18,500*	1.778	>1.000	>1.000
(8)	120	1.00	892	14,900	0.552	0.964	0.532
(9)	275	1.36	656	10,500	0.348	0.500	0.174
(10)	462	1.58	565	8,900	0.231	0.360	0.083
(11)	720	1.72	519	8,100	0.162	0.300	0.049
(12)	1035	1.78	501	7,800	0.117	0.280	0.033
(13)	44	1.00	892	18,500*	1.338	>1.000	>1.000
(14)	160	1.02	875	14,600	0.423	0.926	0.392
(15)	365	1.48	603	9,600	0.286	0.416	0.119
(16)	617	1.68	531	8,400	0.184	0.324	0.060
(17)	960	1.77	504	7,900	0.125	0.288	0.036
(18)	1380	1.79	498	7,800	0.088	0.280	0.025
(19)	55	1.00	892	18,500*	0.938	>1.000	>1.000
(20)	200	1.20	743	12,400	0.398	0.668	0.266
(21)	455	1.58	565	9,000	0.244	0.366	0.089
(22)	770	1.73	516	8,100	0.152	0.300	0.046
(23)	1200	1.79	498	7,800	0.101	0.280	0.028
(24)	1725*	1.74	513	8,000	0.069	0.296	0.020

*Extrapolated

**Column 4 is based upon a working stress of 20 ksi and F_{max} = 22.42 psi producing σ_w/F_{max} = 20,000/22.42 = 892.

VI. CONCLUSIONS

It can be seen from the sample calculations that there are a number of cases that would be acceptable for design purposes. In general, when a resulting stress is considerably larger than the design limit, the corresponding deflection is also unacceptable. A comparison of Tables 4 and 5 shows zircaloy to have lower stresses but larger deflections than stainless steel. The additional stiffness of the cellular plate, resulting in smaller deflections than those for a solid plate, is evident in Table 7.

Since these calculations are generally conservative from the approximations used in the analyses, it follows that there should be no difficulty developing a satisfactory design for such a substructure.

Acknowledgment

This work was supported by Sandia Laboratory, Albuquerque, NM, under contract to the United States Department of Energy.

REFERENCES

1. Szilard, R., "Theory and Analysis of Plates," Prentice-Hall, Inc., New York, 1974.

2. Bares, R., "Tables for the Analysis of Plates, Slabs and Diaphragms Based on Elastic Theory," 2nd ed., Bauverlag GmbH., Wiesbaden, 1971.

3. Biggs, J. M., "Introduction to Structural Dynamics," McGraw Hill, Inc., 1964.

4. Peterson, R. R. and Moses, G. A., "Blast Wave Calculations in Argon Cavity Gas for Light Ion Beam Fusion Reactors," UWFDM-315, University of Wisconsin (October 1979).